Project Summary/Abstract

Targeting dose to submillimeter or subdegree accuracy to tumors in a patient's target volume while simultaneously sparing organs at risk (OAR) is crucial for successful tumor control. A critical component of this process is image-guided radiation therapy (IGRT) that allows the localization of tumors and OARs while a patient lies supine on a treatment table. Currently, computed tomography (CT) images are employed in segmenting critical structures from organs-at-risk (OARs) in IGRT. However, CT images exhibit low delineation contrast for the soft tissues of brain and head-and-neck (H&N) region. Magnetic resonance imaging (MRI) is the most effective imaging modality that provides a clear-cut visualization of tumors and OARs. MRI provides real-time imaging characteristic for tracking anatomical motion for MRI guided RT and for dose reconstruction as well as real-time image adaptation.

Research organizations such as the University Medical Center Utrecht and Viewray have demonstrated the feasibility of simultaneous MR imaging and irradiation from linear accelerators and there now exists clinical prototypes. However, when the patient lies supine on the couch, intracranial head motions can cause MR imaging artifacts – limiting the effectiveness of MR imaging; even so, head excursions beyond an acceptable tolerance can cause damage to critical structures, sometimes resulting in eczema and other brain injuries. The state-of-the-art mechanisms for keeping the head static in clinics are rigid Brown-Robert-Wells head frames or thermoplastic face masks. However, patients find these devices inconvenient, and highly invasive. Furthermore, they cause poor patient compliance to prescribed radiation dose and they cause clinical inefficiencies.

In my previous investigations, I have shown the effectiveness of soft robots at head motion correction up to submillimeter accuracy in lower task-space dimensions. My hypothesis is to use a soft manipulator, actuated from compressed air, and adaptable to the confined space under MR coils so as to eliminate the motion artifacts caused by involuntary head motions. I will develop a motion-planning algorithm and construct an $\mathbb{SE}(3)$ task space soft robot for real-time patient head motion correction in MR machines and MRI-linear accelerator treatment procedures. When this has been tested on phantoms and human volunteers, I will validate its suitability in human trials in the independent years of this proposed project.

Project Narrative

Accurate dose targeting to malignant cancers in radiation oncology requires a versatile delineation of soft tissues within the target volume in order to tell critical structures apart from organs-at-risk. Currently, CT images are used in this segmentation task which lack and the required delineation capability. MRI provides real-time imaging characteristic for tracking anatomical motion for MRI guided RT, dose reconstruction, as well as real-time image adaptation. This project will leverage the high-contrast that magnetic resonance scans provide with the non-magnetic and radio-transparent compliance that soft robots provide in cranial position manipulation so as to assure better clinical outcomes for head and neck (H&N) as well as brain cancer treatments in integrated MRI-LINACs radiation therapy treatment procedures.

Candidate's Plan to Provide Mentoring

I have carefully chosen my mentor and co-mentors to reflect the needs of the aims articulated in this proposal. Taken together, the respective expertise described in this proposal span (i) robust adaptive optimal control; (ii) motion planning; (iii) mechanics of materials; (iv) continuum mechanics/elasticity theory; (v) soft robots fabrication; and (vi) medical physics. No team is better able to mentor me on these subjects than Professors George Pappas, Kevin Turner, James Pikul and Rodney Wiersma.

Professor George Pappas

Professor Pappas is the UPS foundation Professor at the University of Pennsylvania. He holds a principal appointment in the Electrical and Systems Engineering Department and has cross-appointments in the Computer and Information Science (CIS), as well as Mechanical Engineering and Applied Mechanics (MEAM) departments. He has made pioneering contributions to the analysis, design, and control of cyber-physical systems with applications to safe and secure autonomy. Dr. Pappas developed an award-winning theory of hierarchical model approximation across continuous-time control models, discrete-event software models, and hybrid systems (cyber-physical models) which resulted in a paradigm of approximate symbolic abstractions for continuous and hybrid control systems, bridging together semantically continuous-time and discrete-event systems. He subsequently leveraged his approximation theory in order to develop the first rigorous theory of robustness for temporal logic safety specifications and analysis for continuous control systems.These foundational and influential achievements enabled the development of numerous safety analysis and synthesis tools by the cyberphysical systems community. The emerging field of semantic SLAMs was invented by him. I will be relying on his deep control theory expertise, and project management prowess in successfully executing K_{99} *Aims II and III* described in this proposal. He has graciously accepted to continue to provide mentorship and supervision of my career development during the independent phase of this award. As we are physically located on the same campus, I will ensure that I meet with him at least twice a month to discuss my progress on this project as well as continually seek his mentorship on navigating the junior academic hurdles that I may encounter as my career develops.

Professor Kevin Turner

Professor Turner is the Professor and Chair of the Mechanical Engineering and Applied Mechanics (MEAM) at The University of Pennsylvania. His research addresses fundamental and applied problems at the intersection of surface/interface mechanics and micro/nanosystems. His research group uses a combination of experimental measurements, analytical modeling, and numerical simulations to improve and realize innovative micro- and nano-manufacturing processes as well as to develop new approaches to measure the mechanical properties of interfaces at small scales. I will be using some of the instrumentation available in MEAM and Professor Turner's lab in executing K_{99} Aims I and III during the mentored phase of this project. MEAM houses Penn's Rapid Prototyping Laboratory (RPL), ADDitive Manufacturing Laboratory (ADDLab) as well as Dr. Turner's laboratory. These laboratories offer state-of-the-art additive manufacturing capabilities such as soft lithography 3D printers as well as general-purpose mechanical engineering instrumentation such as moduli testing machines. In addition, Dr. Turner will provide supervision and guidance in the continuum mechanical model and adhesives development at the interface of the robot and human head during the construction of the proposed robot. Given his excellent administrative expertise, Dr. Turner will coach me on job talks, laboratory management and I will meet with him and his research group at least twice a month.

Professor James Pikul

Professor Pikul is an Assistant Professor at Penn's MEAM. Professor Pikul is a mechanical engineer by training with expertise in materials engineering, micro and nanoscale fabrication, soft robotics, and electrochemistry. His group combines these expertise to enable new robotic capabilities. He recent patent and publication in Science demonstrates a new physical approach for controlling the shape transformation of stretchable material surfaces, in an engineered system that provides reversible actuation, fast response, large forces, geometric and sequential control, as well as ease of fabrication. Specifically, Dr. Pikul will be responsible for the supervision of hardware fabrication of the soft robots and guide with mentoring support in NSF-style grants writing.

Professor Rodney Wiersma

Professor Wiersma is an Associate Professor at Penn's Department of Radiation Oncology as well as the Director of Physics Research in the department. Dr. Wiersma has been at the forefront of robot-based radiation therapy since he was Assistant Professor at the University of Chicago. His research group was the first to demonstrate the capability of a rigid 6-6 Stewart-Gough platform to correct patient head motion in real-time on human volunteers in stereotactic radiosurgery. Dr. Wiersma is my current postdoc advisor. In the mentored phase of this award, he will oversee the execution of this project. While I will be responsible for project execution, Dr. Wiersma will actively help with the coordination with other co-mentors in terms of joint lab meetings, mentoring, laboratory management, and grants writing.

Specific Aims

Integrating magnetic resonance imaging (MRI) functionality with radiation therapy (RT) linear accelerator (LINAC) can better render the visualization of the soft tissues of lesions and surrounding healthy organs-at-risks (OARs) during cancer RT treatment planning and procedures. This is because MR scans, in contrast to the prevalent computed tomography (CT) scans used in clinics today, provide a richly contrasted image of internal body tissues. More importantly, MRI-LINAC integration can be done in an unrivaled, online, and real-time fashion to aid a more precise radiation dose delivery in RT [1]. However, the quality of MR scans are limited by head motion artifacts. Given the consistency of head motion requirement for proper beam targeting in stereotactic radiosurgey (SRS) and highly conformal head-and-neck (H&N) RT, rigid head frames or thermoplastic face masks are currently clinically used as static head immobilizers. However, frames are uncomfortable and highly invasive – causing poor patient compliance and clinical inefficacy; and masks reduce dose targeting accuracy – since mask flex can lead to drifts of up to 6 mm from an intended target. Robot mechanisms for real-time head motion correction that have been investigated are made out of linear actuators and rigid metallic components which are incompatible with MR [2–4]. During my PhD, I used soft manipulators for head motion correction in RT treatment planning in lower task space dimensions. Here, we propose a novel non-magnetic and radiation-transparent soft robot for automating the online, real-time patient head motion correction in emerging MRI-linear accelerator (LINAC) RT treatment procedures. Our team, comprised of material mechanics, medical physics, control systems and soft matter experts, will address these issues via the following specific aims:

K99 Aim I: To Develop a Distributively-Innervated, Non-magnetic, and Radiation-Transparent Soft Actuator.

My preliminary soft manipulator designs have been used to control H&N motion in RT for up to 3 DoFs. This aim will scale my previous designs to a fully parallel soft robot capable of providing head manipulation along 6 DoFs and will be integrable with pre-existing LINACs. The actuators will be fiber-reinforced to constrain deformation along specific Eulerian directions in order to simplify control. Made entirely out of radio-transparent and non-metallic parts, this Gen 2.0 design will be adaptable under MR coils and the large tubular MR magnets and hence suitable for patient head motion compensation in emerging MRI-LINAC treatment procedures. A hierarchical sensing and control scheme is proposed: the soft actuators will deform in a manner similar to the fast activation ($\leq$2secs) of, for example, the papillae of the octopus, and will have rich surface innervation (e.g. similar to the cuttlefish skin) to aid rich system state perception; this will enable accurate feedback control of the pressurization within the actuator's air chambers. *We expect that this bleeding-edge application will demonstrate for the first time that soft actuators can excel at precise deformation schemes that are safe and compliant for real-world medical applications.*

K99 Aim II: To Develop a Multi-Modal and Robustly Stable Optimal Motion-Planner.

Our preliminary results show the need for a head manipulation motion planner that is safety-aware for executing optimal collision-free paths between transition modes such that manipulating the patient's head does not expose normal brain tissues to high radiation doses. This aim will find a robustly stable and optimal head motion trajectory for moving the head from a start location $\xi_i \in SE(3)$ to a goal location $\xi_f \in SE(3)$ safely. As the desired head motion is continuous with discrete underlying structures, the manipulation problem is multi-modal with a continuous admixture of modes. The current convention in robotics is to use layered planning whereby search is hastened by solving a planning problem at various abstraction levels. However, such planners often miss stability-guarantees in their optimal path formulations hence resulting in paths that are not stably robust for assuring safety in the execution of planned paths. *We will address the current gap in geometric manipulation problems under manifold constraints that leave out stability analysis by leveraging an asymptotically stable robust control Lyapunov function optimally stable motion-planning feedback controller in order to safely generate optimally-robust single modes that guide transitions that precisely move the head in the presence of medical constraints in the head-robot workspace.*

K99 Aim III: Mechanism Assembly, Phantom, and Healthy Volunteer Experiments.

A soft robot mechanism will be constructed, able to fit under the MR coils and able to (re)position the patient as needed during treatment. In addition, a 3D surface imaging sensor will measure patient's head position and feed it to the motion planner's head position feedback controller. Patient safety systems based on automated treatment beam shut off will be incorporated into the finished design. The motion-planner in K99 Aim II will be used in the real-time head motion correction in mock MRI-LINAC RT phantom and healthy human volunteer experiments. An end-to-end testing with 3D-printed head phantoms containing dosimetric gel will be used to evaluate 3D radiation dose accuracy for both single and multiple target SRS plans. A 20 volunteer study with a mock radiation beam will be conducted in a clinical environment to verify linear and angular head position control and patient safety systems.

R00 Aim: Patient Oncological Clinical Trials.

A clinical trial on 20 whole brain patients will be performed where validation of this system will be determined by a statistical endpoint. Success will be that a 6D intracranial target is $\leq$ 0.5mm and $\leq 0.5°$ for greater than 95% of the treatment time. Upon successful completion and novel use in in maskless MRI-LINAC systems, this project will demonstrate that soft robotic SRS is ready for widespread clinical deployment. With its transformational clinical potential, our soft robot head motion compensation in MRI-LINAC RT will enable the availability of novel radiation dose delivery to a larger population of patients, improve therapeutic outcomes, reduce patient invasiveness, improve clinical efficiencies by reducing current setup times from hours to minutes, and will be compatible with thousands of pre-existing LINACs.

Future Plans: ***I plan to expand this project into my own independent research laboratory where I will study to design and control soft robots for broad biomedical engineering applications in human-robot interfaces.***

Research Strategy

Significance

Integrating magnetic resonance imaging (MRI) functionality with radiation therapy (RT) linear accelerator (LINAC) can better render the visualization of the soft tissues of lesions and surrounding healthy organs-at-risks (OARs) during cancer RT treatment planning and procedures. This is because MR scans, in contrast to the prevalent computed tomography (CT) scans used in clinics today, provide a richly contrasted image of internal body tissues. More importantly, MRI-LINAC integration can be done in an unrivaled, online, and real-time fashion to aid a more precise radiation dose delivery in RT [1]. There are now MRI-LINAC systems such as Raaymakers et al's [1,5], which was later commercialized by Elekta AB (Sweden) [1].The MRIdian system is another one of such technologies, essentially an MRI-based image-guided RT [6], developed by Viewray (USA). There is also the Aurora RT system from MagnetTx (Canada) [7], or the non-commissioned Australian MRI-Linac project [8]. While MRI-LINAC integration has been widely researched [1, 5, 9, 10], the effect of random and involuntary patient motion causes motion artifacts which lowers the quality of MR imaging scans for use in brain and head and neck (H&N) RT. These artifacts in image collection lower the accuracy of online and real-time precise radiation dose delivery, which in turn affects clinical efficacy.

During RT, it is paramount to keep the patient accurately positioned on the treatment table, especially in applications aimed at more precise irradiation such as in head and neck cancers. The importance of accurate patient positioning is further underscored by accumulating evidence that patient displacement and collimator and gantry angle misalignment during RT showed high sensitivity to small perturbations: a 3-mm error in anterior-posterior direction caused 38% decrease in minimum target dose [11].Thus, to automatically align patient motion during RT, state-of-the-art clinical approaches use either a frame or a mask to stabilize patient motion on the treatment couch.

Known roles of frames in positioning compensation

In frame-based approaches, a metal ring (the Brown-Robert-Wells frame) is attached to the patient's skull using screws, and then bolted to the treatment table, Fig. 1a. Discomfort and severe pain often results from long hours of minimally invasive surgery where the skull is fixed with pins for head immobilization during stereo-tactic radiosurgery (SRS). The invasiveness and discomfort associated with the frame are a principal cause of poor patient compliance and poor clinical efficacy. For some patients, frame placement is not feasible due to extreme cranial anatomy or prior surgical bone flaps. In cases where multiple radiation therapy (RT) deliveries are needed, patients cannot be subjected to daily attachment and removal of the frame.

Known roles of masks in positioning compensation

These limitations of frames have spurred clinics to start using thermoplastic face masks. Here, a porous mask is deformed to fit the geometry of the patient's head and neck region and then fastened to the treatment table. As the mask is flexible, during the course of treatment, it loses its firmness around the patient so that the inaccuracy of dose targeting is inevitable. The flexibility of masks has been identified to cause a drift of up to 6mm. This is unacceptable given the AAPM TG-42 positioning accuracy guidelines that specify < 2 mm accuracy [14]. Changes in the mask's physical texture from repeated application and shrinking, Fig. 1b, can also lower treatment accuracy. These inconsistencies are not suitable for deep tumors located nearby critical structures such as the brain stem or for newer treatment modalities such as single isocenter multiple-target SRS, which are highly sensitive to rotational head motions. Even so, conventional LINACs used at most cancer centers are insufficient for the high geometric accuracy and precision required of SRS for isocenter localization [15].

Known roles of rigid robots in positioning compensation

To overcome these issues, explorative robotic positioning research studies have demonstrated the feasibility of maintaining stable patient cranial motion consistent with treatment plans. For example, the Wiersma Lab's Stewart-Gough (SG) platform [2, 16, 17], illustrated in Fig. 1(c), achieves ≤ 0.5mm and $\leq 0.5°$ positioning accuracy 90% of the time. It is constructed as a 6-6 SG platform out of linear

(a) The BRW SRS Frame [12] *(b)* Frames with MRI Coils *(c)* Wiersma SG-Robot [13] *(d)* Ostyn's Stewart platform [4]

Figure 1: Existing frame and mask (a-b), and frameless and maskless robotic systems (c-d).

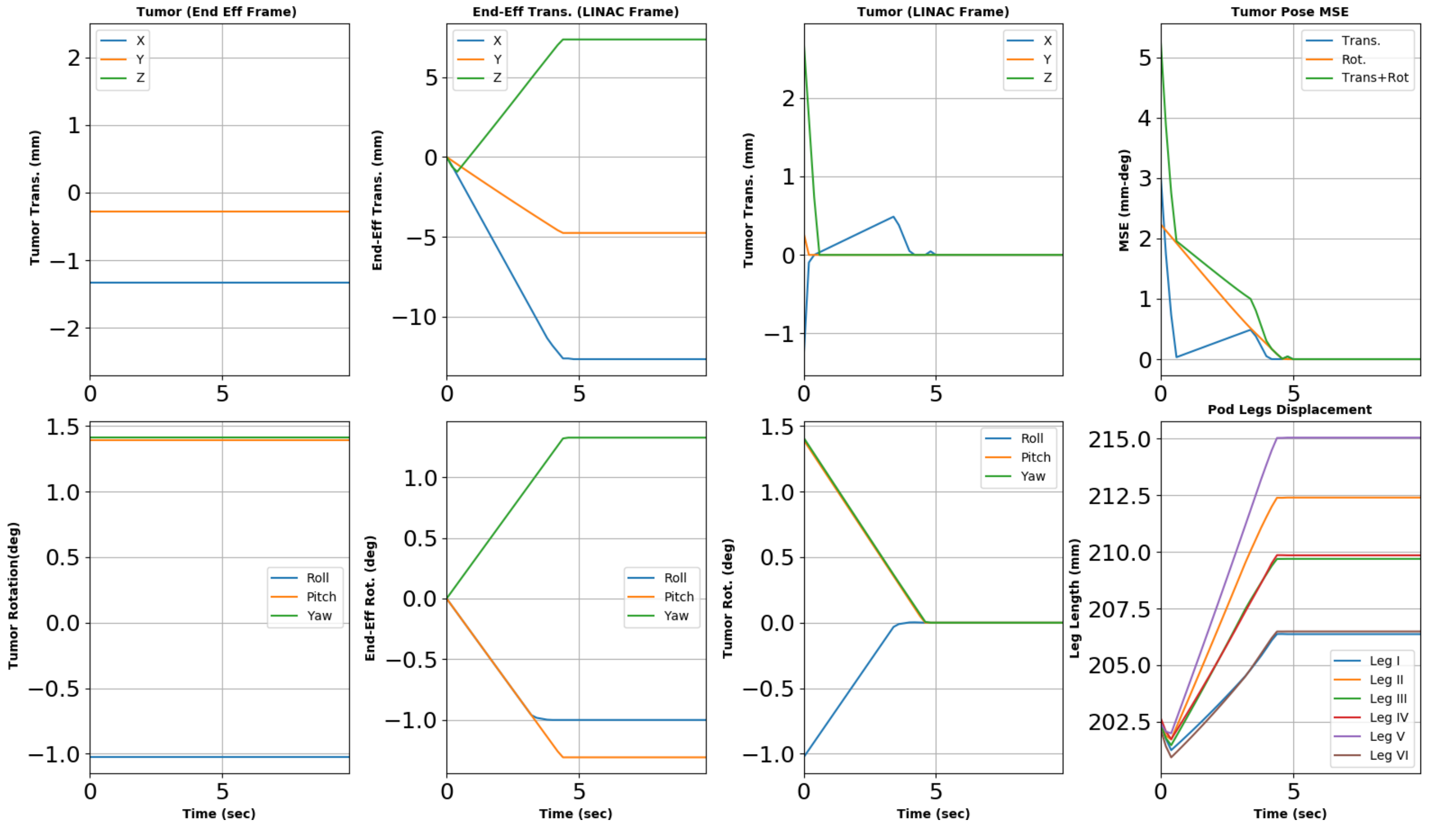

Figure 2: Isocenter Head Stabilization Results Using the Wiersma Rigid Stewart-Gough Platform. Reprinted with permission from [17].

actuators, electric motors and rigid metallic components. While effective at head position compensation in SRS treatment procedures, it is not adaptable for new MRI-integration with LINAC RTs that offer better real-time soft tissues delineation for a precise irradiation. The Ostyn et al research group sought to alleviate this rigid structure by 3D printing the mechanical components of the Stewart-Gough platform [4]. It is worth noting, however, that this platform uses stepper motors as well (see Fig. 1(d)) to actuate the legs of the robot. This by nature leads to radiation attenuation. With the potential to aid better clinical accuracy in SRS-based systems when commissioned, these systems are not suitable for the emerging MRI-LINAC machines. This is because they utilize rigid metallic components, electric motors and linear actuators which are not suitable for the large tubular magnets of the MR machine: they interfere with the magnetic fields of the MR machine and have been known to lead to patient fatality or significantly damage the MR machine when clinicians have been careless about bringing metallic materials into the treatment room [18].

Published work from the Wiersma lab shows that a rigid parallel robot can provide the online, real-time patient motion compensation in mock SRS and RT treatments (see Fig. 2). Here, using an LBFGS-based trajectory optimization formulation for patient head motion compensation, the algorithm was able to maintain a ≤ 0.5mm and $\leq 0.5°$ clinical tolerance objective for 100% of the treatment time [17]. But observe that not all constraints are adhered to: for example, observe the overshoot along Z for the tumor in the LINAC frame and the wriggly trajectories along the rotational axis of the tumor before it reaches steady state. Furthermore, while this robot does work well for SRS treatment procedures, it does not translate to integrating MRI functionality with LINACs owing to its structural mechanical characteristics.

Known roles of soft robots in RT

My preliminary work on soft manipulators for patient head motion compensation in RT shows that novel soft robot manipulators can compensate head motion within the submillimeter and subdegree accuracy of the AAPM-TG42 stipulation for up to 3 DoFs [19–22]. In a cascaded PID-PI controller loop, I initially showed head motion correction for head setpoint- and trajectory-following to be accurate to within $\leq$ 1.5mm for a task of lowering or raising the head along on a treatment table [19]. These results are duplicated in Fig. 3. Furthermore, Fig. 4 illustrates the testbed I used in generating the 3-DoF control results of Fig. 5. Here, the setup consists of a phantom with a neck simulator that models the ball joint in the human torso. A vision-based 3D sensor acquires the face's point cloud in real-time, which is then processed for features-extraction and the 6D coordinates of the head (here using the tip of the nose) are sent to a microcontroller (National Instruments®myRIO); the myRIO then regulates the flow of compressed air into a set of proportional solenoid valves. The amount of air within the set of inflatable air bladders (IABs), in turn raise, lower, or tilt the head on the mock treatment table. The dynamics of the head interaction with the IABs and air pressure supply were carried with a lumped prediction error model [23].

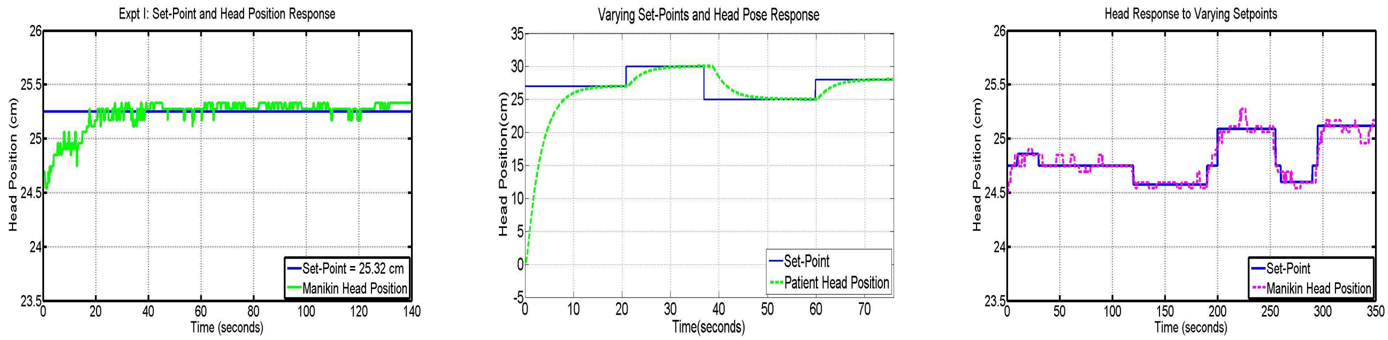

(a) Head response to fixed setpoint. *(b)* Head trajectory follower simulation *(c)* Head trajectory follower experiment

Figure 3: 1-DoF Online, Real-Time Head Motion Correction. Reprinted from [19].

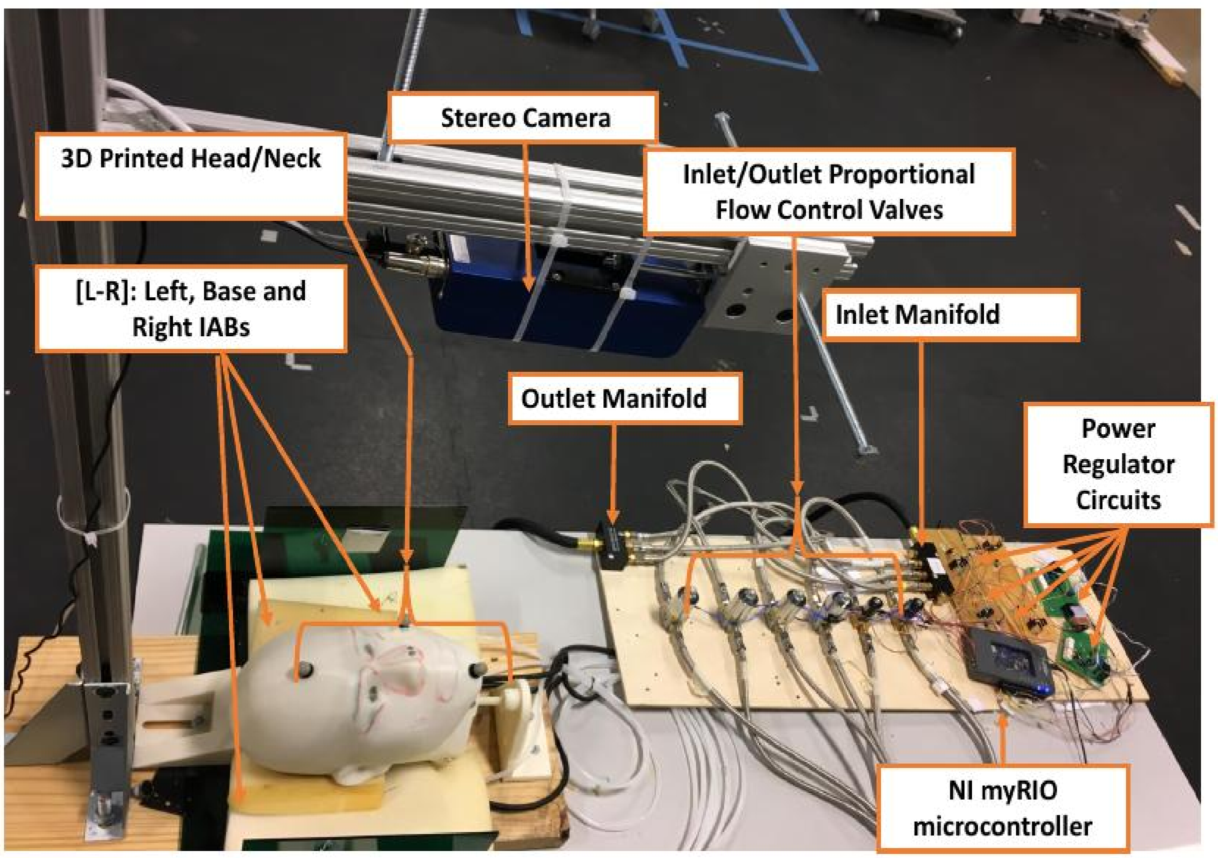

Figure 4: Three DoF Testbed. Reprinted from [20].

This model was then used in a controller that leveraged indirect model reference adaptive control with optimal state regulation in order to ensure the head follows set trajectory through steady-state [20]. Some of these results are reprinted in Fig. 3 and Fig. 5 respectively.

Now, in a new class of soft actuator designs, and contrary to stochastic system identification techniques I used in my previous models [19,20,22], we can now specifically regulate volume fractions within the IABs as well as accurately control their spatial deformations based on specific nonlinear elastic deformation relationships [24]. Being continuum, compliant and configurable (C3) for manipulation tasks, we recently demonstrated in control experiments that they are well capable of providing patient head motion compensation [13]. Contrary to remote-controlled airbags that have been used in upper mandible and head manipulation [25], our actuators deform based on their material moduli, compressed air pressurization and incompressibility constraints when given a reference trajectory. To our knowledge, ours are the first to explore C3 materials as actuation systems for cranial manipulation in robotic radiotherapy. Deforming based on prescribed internal pressurization, their surface displacement errors are accurate to the order of $< 1.5 \times 10^{-}4$mm [24]. These results are reiterated in Fig. 6 where a spherically-textured soft actuator was prescribed to deform from an initial internal radius, $R_i = 2.7$mm from

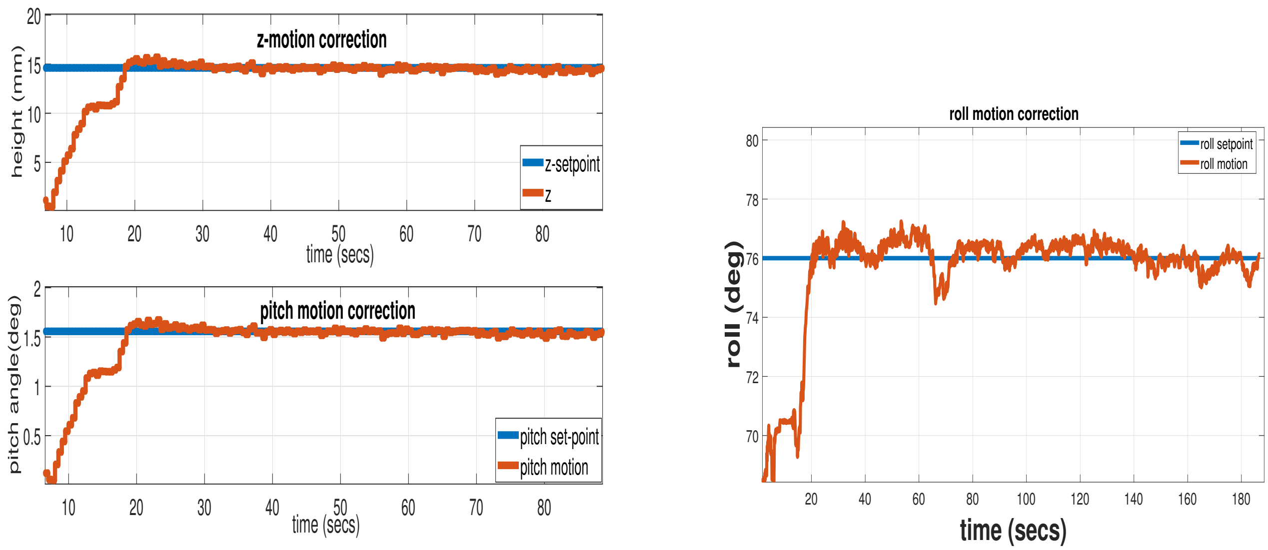

(a) Z and pitch motion correction. *(b)* Roll motion correction.

Figure 5: 3-DoF Online, Real-Time Head Motion Correction. Reprinted from [20].

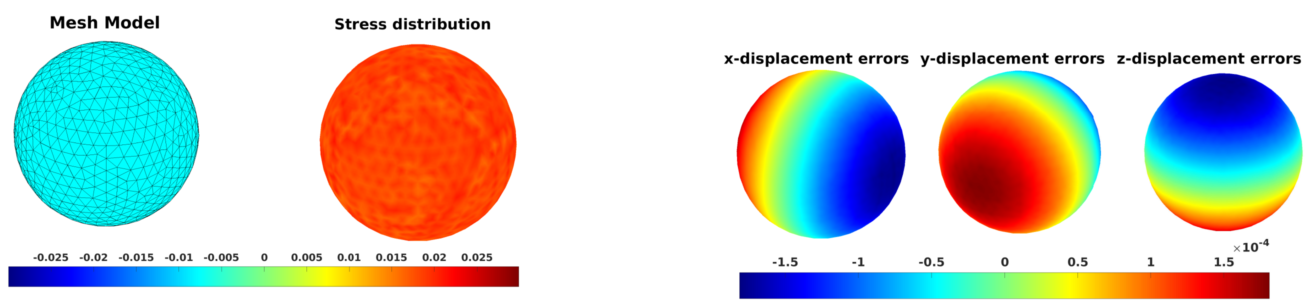

(a) **Left**: Mesh model. **Right**: Stress distribution post-defomation. *(b)* Displacement errors along x, y, z coordinates.

Inputs					Outputs		
C_1	C_2	$R_i(mm)$	$r_i(mm)$	$R_\circ(mm)$	$r_\circ(mm)$	$P(psi)$	ΔV
$1.1e4$	$2.2e4$	2.7	3	3	3.3	.76	$\approxeq 0$

Figure 6: Volumetric Deformation of a Soft Actuator (Expansion). Reprinted from [24].

the reference configuration to $r_i = 3.3$mm in the current configuration. Based on my derived constitutive relation between the applied pressure and the radius of the actuator, a pressure of 0.76 psi was found to be suitable to realize this deformation. The charts of Fig. 6 illustrates the response of the actuator based on a prescribed pressure, where C_1 and C_2 are appropriate material moduli. With the standard local volume preservation principle, we notice a displacement error of 1.5×10^{-4} along the rectangular Cartesian coordinates and a zero volumetric change$i.e.$ $\Delta V \approxeq = 0$. This shows that with *highly accurate pressure sensors*, and equipped with properly calibrated proportional solenoid valves, we can regulate the air within a soft actuator's chamber so that specific and highly precise deformation behaviors are realizable for consumer soft actuators.

Hypothesis

My **leading hypothesis** is to use MRI/LINAC-compatible soft robot system that can provide 6-DoF head motion correction in precision RT procedures to serve as a viable alternative to current mask-based as well as frameless and maskless robot-based cranial manipulation systems. In this sentiment, ***I hypothesize*** *that time-resolved MRI-LINAC techniques, which provide superior soft tissue scans, in conjunction with non-magnetic and radiation transparent soft robots can provide superior brain or H&N radiation dose targets for precise MRI-LINAC RT treatment procedures*. Existing frame-based immobilization devices, Fig. 1a, and frameless and maskless rigid robotic motion correction mechanisms, Fig. 1c&d, are not suitable for this because of their electro-mechanical parts that introduce serious safety concerns. Furthermore, ***I hypothesize*** *that an asymptotically stable in the large and optimal motion-planner can find collision-free paths* *that satisfy head motion constraints can resolve the abnormalities inherent in current controllers used in head motion correction systems [2, 3, 16, 20], This will alleviate the overshoots experienced during head motion correction as illustrated in Fig. 2*. I will test this leading hypothesis to see if 6-DOF target motion of a patient is ≤ 0.5 mm and $\leq 0.5°$ for greater than 95% of the treatment time using MRI imaging for soft robot-based motion compensation.

Along with other experiments where I verified that vision-based control of soft robots can geometrically correct patient motion precisely fast-enough in real-time up to three DOFs [19–22], and existing hybrid MRI-compatible RT systems [5, 9, 10], we will test these hypotheses that soft robots can provide position accuracy that is consistent for use in standalone MRIs, MRI-LINAC RT systems or SRS-alone treatment procedures in order to (i) negate the deleterious effects of *interfractional* setup variation on patients; (ii) correct the complex *intrafractional geometric uncertainties* such as posture changes, and body deformation with minimal invasiveness; (iii) eliminate radiation attenuation associated with the metallic components of frames and rigid robotic patient motion compensation systems; and (iv) correct the flex associated with thermoplastic face masks; (v) reduction of radionecrosis. Typically, a radiation oncologist typically adds a 1-3mm volume margin around the tumor to ensure adequate radiation dose coverage in the event of head motion. This exposes more brain tissue to radiation and greatly increases the risk of radionecrosis. The mechanism has the potential to significantly reduce these margins and therefore improve therapeutic outcomes. while *not interfering with the MR machine's magnetic field*.

Innovation.

Conceptual Innovation

My work was the first to demonstrate the feasibility of vision-based 3 DOF control of soft manipulators for cranial motion management in RT [19–22]; we are extending this to 6-DOF control with my novel advanced mechanism

- The newly proposed mechanism is made entirely of no metal (hence not susceptible to magnetic fields) and is radiation-transparent so that it is compatible with MRI-LINACs RTs and SRS. It would be compatible with all 15000+ pre-existing LINACs worldwide. This would include conventional L-arm (Elekta, Varian), robotic arm (Cyberknife), and ring-type (Tomotherapy) LINACs. It would be implemented as a standard treatment table accessory that can be easily attached and de-attached from the end of the table and would not require costly room modification or other dedicated equipment. Since it is likely to be inexpensive, it has potential to bring state-of-the-art RT methods to developing nations with older LINAC technologies.

- This mechanism can be adapted to confined spaces under MRI coils (see Fig. 1b) given its compactness, and light weight.

- Increased clinical efficiencies. It possesses little invasiveness to the patient, and exhibits a quick-connect, quick-disconnect modularity on a couch – important for patients with varying cranial anatomy – thus easing the logistical setup workload of current immobilization and maskless robotic systems. As current SRS setup procedures are highly complex, expensive, and can require support from highly trained medical staff such as neurosurgeons. Total in-clinic treatment times can range from 68 hours. Soft robotic MRI-LINACs in RT and SRS will significantly cut down on the setup complexities and time required to perform SRS as a neurosurgeon is no longer required for frame placement or the construction of specialized thermoplastic masks. Instead of hours, treatment setup time will be reduced to a few minutes, as the patient lies down and the robot quickly adjusts to bring the intracranial target to the correct position.

- Less invasion to patients than current frame or frameless SRS systems. The soft robotic SRS will not require a frame or mask around the patients head. The only requirement is for the patient to lie down on a soft foam headrest. Advanced optical guidance systems will then detect positional deviations and the robot will make automated head corrections.

Technical/Healthcare Innovation

To our knowledge, **no currently-available technology exists today that can perform real-time head position stabilization *without dose attenuation* in an online, real-time fashion whilst guaranteeing patient safety similar to our proposed MRI-LINAC non-magnetic and radio-transparent soft robot RT positioning system**. The superior image guidance from an MRI scan will improve positioning accuracy and irradiation efficacy via a real-time 6D motion-planning control that finds the best 6D trajectory in each head motion transition mode so as to minimize exposure of healthy brain tissues to radiation and adapts to non-rigid body response between the robot and patients head. These soft robotic automatic patient motion compensation systems have broad applications in medical imaging and cancerous tumor management: standalone MRIs, emerging MRI-LINAC technologies, brain RTs and H&N RTs. Throughout the rest of this document, these applications will be broadly referred to as MRI LINACs. As photon-based cancer treatment accounts for $> 50\%$ of all cancer treatments [26], these exploratory experiments are relevant to public health and have transformational clinical potential because they may provide (i) proof-of-concept evidence that soft robots are compatible with standalone MRI imaging modalities; (ii) evidence of precise and automatic motion management with non-magnetic and radiation-transparent soft robots in emerging hybrid MRI-accelerator RT; (iii) an emergence of a better brain and H&N cancer management technology that can be adapted to confined spaces under MRI coils (see Fig. 1b). Upon successful completion, this soft robot will be used for active head motion stabilization within an MR machine. It will be adaptable for standalone MRIs, emerging MRI-LINAC technologies, and brain as well as

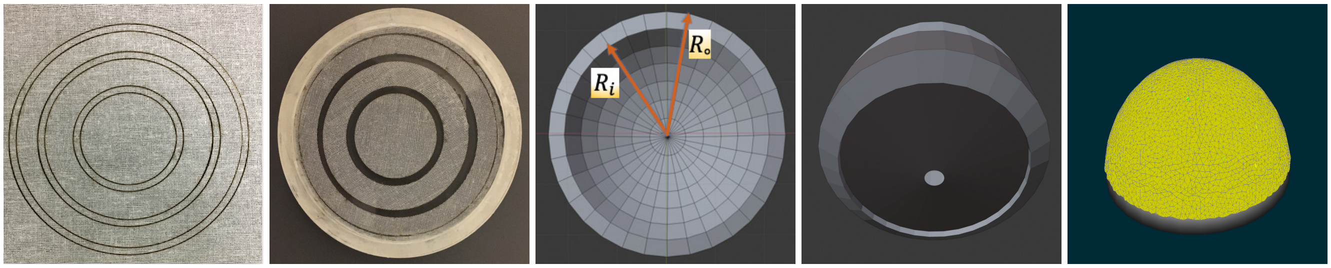

(a) Laser-Cut Fiber *(b)* Fiber+Uncured silicone *(c)* Deformation Model *(d)* Actuator+PVC Base *(e)* Finite Element Model

Figure 7: Soft actuator fabrication procedure.

H&N RTs. It will provide accurate RT beam targeting as well as preventing patient motion MRI imaging artifacts. This technology will improve therapeutic outcomes, and eliminate patient invasiveness.

Approach.

K_{99} Aim I: To Develop a Distributively-Innervated, Non-magnetic, and Radiation-Transparent Soft Actuator.

Rationale: For though the design of Fig. 4 is relevant to head motion control on an RT treatment table, it is not a complete motion correction system owing to its underactuated mechanism: it is only able to correct motion for up to three DoFs. Motion of the head occurs along six DoFs and they are not independent. Therefore, to realize a full patient motion compensation, more actuators are needed in the mechanism. To this end, and iterating further on my previous designs [20–22], I now propose a new class of continuum, compliant and configurable (C3) light, and agile soft actuators [24, 27, 28] which are the composition of a non-magnetic and radiation-transparent soft robot for use in MRI-LINACs to further aid dose delivery precision. The component soft actuators are planar and circular in their reference configuration. Upon compressed air actuation, they deform along the radial direction (see computer model in Fig. 7) based on the physical constraints baked into the elastomer-fabric matrix. This actuation design is inspired by the behavior of the skin papillae of certain Cephalopods (octopus, cuttlefish, bivalves and mollusks) which can transform their physical texture from 2D to 3D in less than 2 seconds [29, 30]. The actuators exhibit a radially symmetric deformation and are constrained along their circumferential axis under pneumatic actuation based on their novel design. There exists no electrical wirings or embedded electronics to assure that the actuators reach a desired configuration.

Hypothesis: Based on previous success of air actuated elastomeric chambers for manipulating patient head motion correction in real-time, I hypothesize that a fully-compliant and parallel soft robot can effectively correct patient head motion (given a robustly stable and optimal controller) such that the motion artifacts that are prone in MR imaging can be eliminated. This will assure an improved RT treatment outcomes in modern MRI-LINAC RTs.

Procedure.

A. Soft Actuator Design: The soft actuator fabrication methodology is illustrated in Fig. 7. A thin-layered fabric is laser cut into circular patterns (Fig. 7a), the cut meshes are removed and laid onto uncured silicone (Fig. 7b) which has been poured into a mold. We further add a silicone topcoat layer to the fabric before we allow it to cure at room temperature. Upon low pneumatic pressurization, the cured rubber deforms, obeying a Circumferentially-COnstrained And Radially Stretched fiber-Elastomer (CCOARSE) property [31] (Fig. 7c). This unique deformation pattern is similar to the way a balloon would stretch along its axial direction if a rope were tied around its circumference. The soft robot, after cure, is laid onto an impact-resistant, low-temperature rigid PVC insulation foam sheet, encased in a carbon fiber material. This aids radiation transparency (Fig. 7d). The finite elastic deformation mesh model of the soft robot for simulation purposes is shown in (Fig. 7e). This proposed fabrication method allows us to rapidly iterate different designs using compressed low air pressure (1-15 psi) that is (i) cheaply available, (ii) environmentally-friendly, (iii) avoids electrical wirings, (iv) is lightweight, and (v) inviscid which will make the soft robot adaptable for MRI-LINAC systems – creating a clean and safe human-robot workspace. As the air inflow into the chambers of the elastomers need to be carefully regulated, we will build current source electronic regulator circuits that proportionally vary the amount of airflow though connecting hoses that lead into the proportional solenoid valves used in earlier experiments [20].

B. Pneumatic System Design: We now describe the integration of the soft actuator design proposed above with the rest of the pneumatic actuation system. This system is illustrated in Fig. 8. A self-contained compressed air canister supplies air at a fixed pressure (e.g. 15 psi) through a firm polyurethane air tubing into a 4-20mA output-M12 pressure transducer plug connection. The choice of pressure transmitter is important owing to the accuracy requirement for air volume within the chamber of the soft actuator. In our experience, the G2 series of pressure transducers from Ashcroft®are an excellent choice for such application as this: it offers a $\pm 1.00\%$ total error band accuracy; being highly configurable, it offers a pressure range that meets our actuation needs and it can be easily integrated into our overall mechanism. The outlet of this pressure transmitter conveys the airflow into a proportional solenoid valve. We use proportioning valves to control the amount of airflow into the actuator's air chamber because of the air flow precision requirement needed to correctly manipulate the head. The outlet of this solenoid valve then leads to the inlet air connector of the soft actuator. The electronic regulating

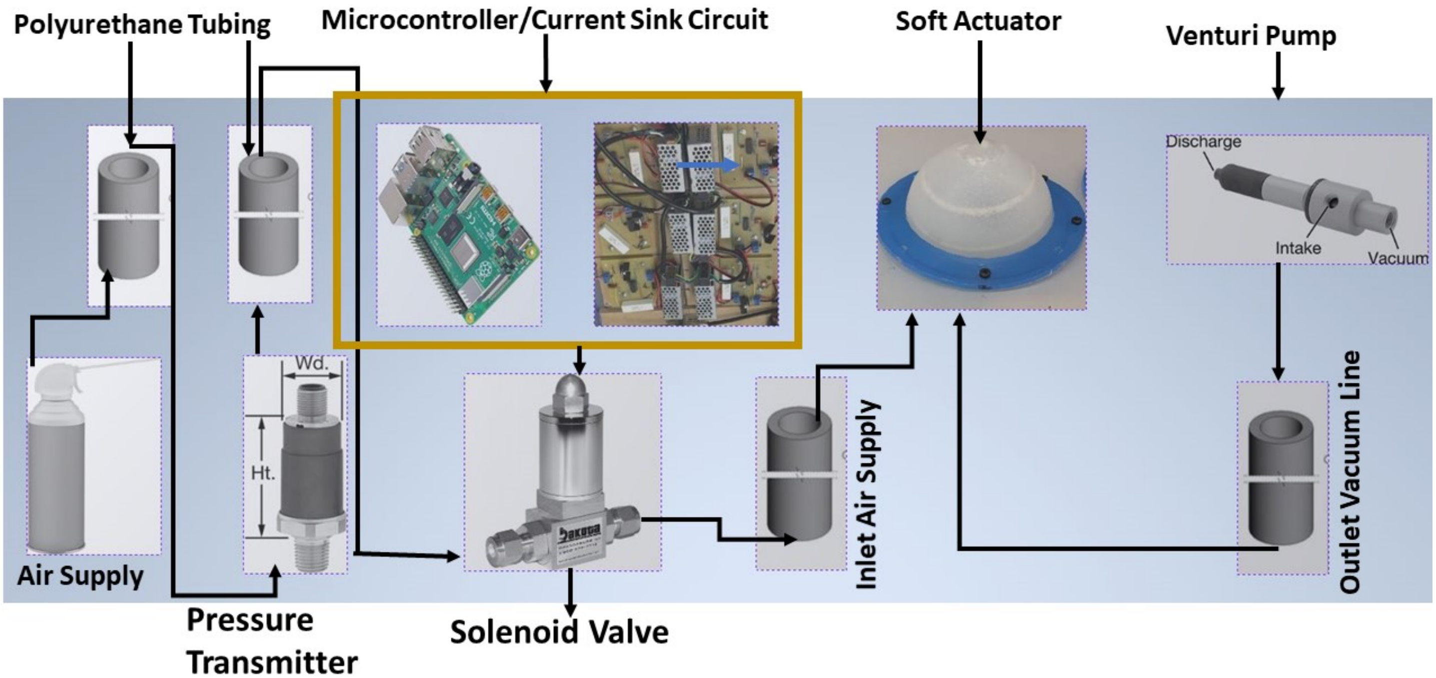

Figure 8: Pneumatic System showing proportional solenoid valve, electronic pressure regulators and raspberry pi microcontroller.

circuit shown in Fig. 8 is a standard current source circuit that varies the air flow rate within the proportional valve by adjusting the current flowing through its shunt resistor. In addition, a venturi pump removes air at a proportional pressure compared to the inlet supply pressure. This pressure differential helps maintain head along a setpoint or follow a varying trajectory.

C. Preliminary Actuation Experiments: We have initial experiments that reproduces deformation behavior similar to the spike observed in the skin papillae of the Octopus. This is described in what follows. We cast silicone from Smooth-On Inc's dragon skin (475 psi tensile strength and 10A shore hardness), whose material properties exhibit enough softness for patient comfort and enough firmness that withstands extremely nonlinear deformation from the wrench produced by the typical human head (55-65 kg [32–34]. The ingrained fabric membrane within the elastomer imposes the CCOARSE property, constraining the circumferential expansion of the rubber and exerting a radially symmetric stretch as shown in the bottom row of Fig. 9. This considerably simplifies the dynamics model that governs the deformation [28]. Two different designs are shown in the top and bottom rows of Fig. 9. The rubber material is screwed onto a bottom PVC foam sheet using a laser-cut acrylic planar ring. We use **nylon** Phillips screws. The behavior at different levels of pressurization are indicated in each column of the figure. The top row shows the cured silicone without fabric while the bottom row shows the silicone with the entrenched fiber matrix within the elastomer. As can be seen, the material in the top row exhibits a circumferential bulge as well as radial bulge while the ones in the bottom row only extend along the axial direction. As can be seen in the bottom row, we can generate a full *Gaussian deformation* and return to the reference planar configuration in 2 seconds (see more images and videos in scriptedonachip.com/soro) similar to the spikes produced by the skin papillae of the Octopus. These quick Gaussian spikes will be useful for rapid head motion correction in MRI-LINACs. The soft compliance and tensile strength of this silicone material make it well-suited for treatment procedures where non-magnetic and radiation-transparent components can boost stereotactic precision as well as improve tumor control in MRI-LINACs.

D. Flexible Piezoresistive Distributed Sensor Integration: In a recent formulation [24], we mapped the relationship between the applied pressure to the deformed radius of a soft actuator using the standard Mooney-Rivlin formulation [35, 36]. Suppose that C_1 and C_2 are appropriate material moduli for the soft actuator, then the applied pressure in the internal walls of the actuator is given by the relation

$$P(r) = \int_{r_i}^{r_\circ} \left[2C_1 \left(\frac{r}{R^2} - \frac{R^4}{r^5} \right) + 2C_2 \left(\frac{r^3}{R^4} - \frac{R^2}{r^3} \right) \right] dr \tag{1}$$

where r_i and $r_\circ$ are respectively the internal and external radius of the actuator walls in the current configuration, and they have corresponding forms R_i and $R_\circ$ in the reference configuration. Taking cues from the precise control schemes of rigid robot manipulators

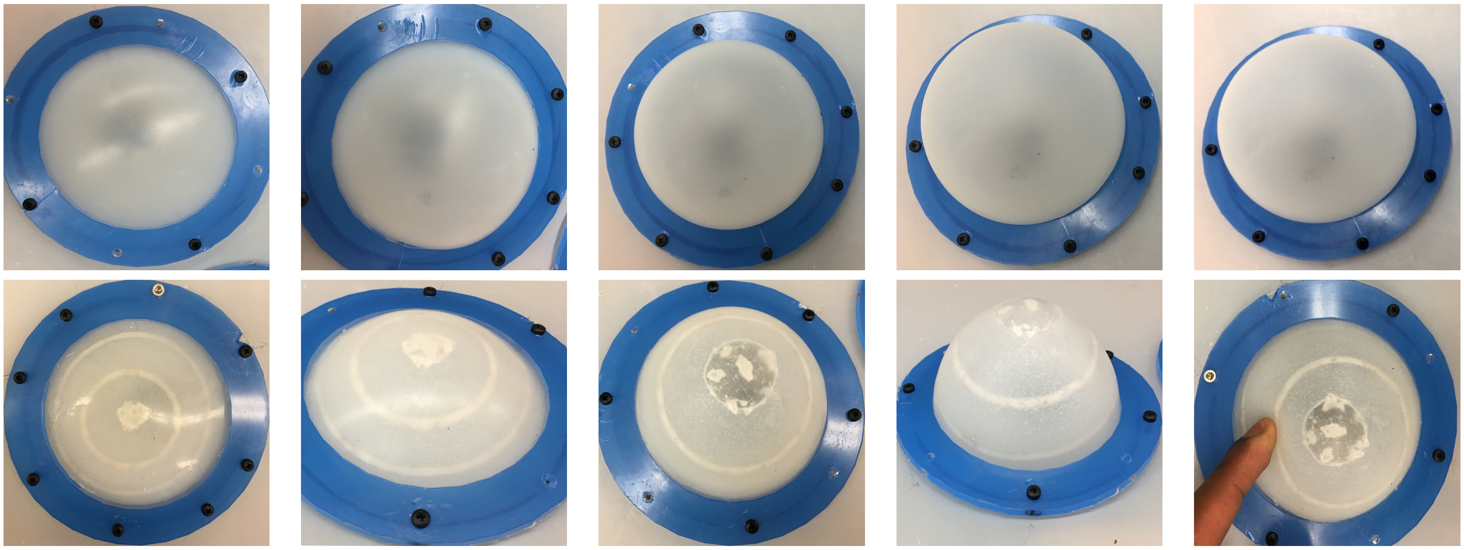

Figure 9: Deformation Levels of elastomer (top) and Elastomeric-Fiber Matrix (bottom) under Low Air Pressurization (3-15psi).

made possible by presence of joint encoders and harmonic drives that enable precise control of the joint angles between robot links, a means of sensing the "measure of deformation" based on the amount of pressure in the actuator's air chamber is necessary for a successful control.

There have been various measures proposed in literature over the past few years about sensing volumetric deformation of a soft actuator. For example, embedded optically-laced fiber sensors based on the principle of frustrated total internal reflection, and distributed throughout a 3D printed elastomer, were used to generate a cointegrated body, sensing, and communication network for a soft robot's state sensing [37]. They have also found applications in innervated soft finger prosthetic hand designs [38], where a very lossy optical waveguide was used in an open-loop control setting to detect shape and texture. While in softness grasp dexterity, they appear promising, they are not yet suitable for human-level texture-based sensitivity (nanometers) despite their complex design. Stretchable sensors with rheological properties have been erstwhile embedded within an elastomer using 3D printing techniques [39]; and though they have been shown to be mechanically receptive, and scalable up to e.g. $\sim$400% strain, their electrical resistance gives at strains $> 400\%$ owing to the percolation of the networked components [39]. Pneumatic actuator networks patterned within an elastomeric robot body via a multi-material, embedded 3D printing technique have been tried [40]. Dielectric elastomers (DE) making use of the static charge properties of passive electronic components have been shown capable of measuring strain by up to 1692% under the Maxwell pressure law [41]. This DE actuators generally rely on electrostatic voltage discharge to sense deformation [42].

Owing to our precise manipulation requirement, a richly innervated means of sensing actuator deformation at high strains (owing to large reactive head forces) is necessary for effective closed-loop feedback control of head motion. Borrowing cues from the observational and short/long-term learning skills arising from the afferent neural networks on the exteroceptive skins of Cephalopods [30, Ch. 2], we will integrate volumetric tactile mechano-receptors on the soft actuators' skins. As we aim to avoid rigid electro-mechanical sources hat can hamper radiation delivery within the design, we will shun DEAs. Optical waveguides would be attractive but they are expensive to integrate for volumetric sensing. Instead, I propose tactile stretchable kirigami sensors made out of polyimides (Kapton sheets) and fiberglass membranes. Meso-scale stretchable Kirigami layer-by-layer manufacture of soft robots have recently been shown to be relevant for fast and precise deployment of robots [43, 44] with high sensing accuracy . Even so, the 3D perception of the environment of these piezoresistive innervated soft robot skins can be perceived using deep learning [45]. In this sentiment, I will laser-cut electrical grade Kapton sheets, weave them in twisting formations with fiberglass materials to mimic the bending of beams that enable accurate sensing [43]. The sensors will then be neatly covalently bonded (without adhesives) to the soft actuators surface by plasma treatment [46]. The proprioception of the soft actuators will be captured by an LSTM deep-learning network such as I used in my previous works [47–49]: this will predict the configuration of each soft actuator during both prescribed and random actuation sequences, even with feedback from non-monotonic, hysteretic, soft piezoresistive sensors. This fabrication approach is attractive because (i) it allows the separation of the fabrication of the soft actuator design from the piezo-resistive sensors; (ii) we can separately characterize the deformation sensing properties of the piezoresistive fiberglass-polyimide sensors for QA purposes before respective integration onto the component actuators; and (iii) it offers a modular and cheap fabrication design methodology that eases troubleshooting during the construction phase.

E. Expected results: I expect to see individual soft actuators obeying the prescribed pressure law given in (1) so that the deformation radius of the actuators exactly follows an applied pressure similar to the presented simulation results of Fig. 6, further elaborated in [24]. In addition, as I am skilled and well-versed in inference using deep-learning methods (see representative publications [47, 48, 50, 51]), I expect that the stretchable Kirigami sensor layers embedded within the elastomeric actuator membranes will produce rich innervated data that can be processed with deep learning based methods [45] for onward control processing.

K_{99} **Aim II: To Develop a Multi-Modal and Robustly Stable Optimal Motion-Planner.**

Rationale: Current SRS-based immobilization and head motion compensation techniques are pre-programmed and heavily calibrated within their environment in order to find the optimal and safest path required in moving a patient's cranial structure from one location to another in the robot workspace [3, 13, 16, 52, 53]. Techniques used range from PID control schemes [2, 19], reduced-order observer feedback control design [22], optimal and robustly stable indirect model reference adaptive control design [20], to local trajectory optimization schemes [17]. While these schemes work manually for specific automation task, they require extensive calibration and adjustment of parameters so as to get them to work in each new environment and for every new head motion control task. For these robots to execute tasks autonomously, a motion planning system capable of generating feasible motion from high-level requirements is needed. In addition, this motion planning system must respect the constraints on a task in order achieve success, such as turning the translating the head about its cranial-caudal axis, or rotating the head about its neck fulcrum. *I will reformulate these control tasks into a manifold-constrained geometric motion planning problem, concerned with finding a feasible optimal and collision-free path for a patient's head motion.*

In order to optimally move the patient's head in an optimally safe and collision-free path that avoids the exposure of normal tissues to high radiation dose, and is not task-dependent, it is important to develop a motion-planner that (i) executes head motion in the robot's workspace by first finding a collision-free path; (ii) improves the plan into a better plan if the original plan is not efficient or does not satisfy C-space constraints; this may involve multiple iterations; (iii) considers how to move the head along a path that is stable and robust for execution in spite of modeling errors and uncertainties, while maintaining various speeds that satisfy various momentum considerations; and lastly (iv) the found plan must be included in a hierarchical planning framework so that the original plan reaches termination, in order to allow larger plans in the hierarchy to roll out as needed. This planing approach is consistent with motion planning algorithms used in robotics [54].

Hypotheses: The requirements produced by this problem and in many other safety-critical problem domains (e.g., household caretaking, IMRT, assistive robots in epileptic patients, and disaster recovery) motivate the study of safety-aware motion planners with constraints. Therefore, **I hypothesize that a layered planning algorithm will find a hierarchical multi-planning sequences of motion that biases search into *optimal mode* transitions**. This layered composition of plans will first compute collision-free paths $\mathcal{C}_{free}$ for moving the head between the start and goal poses. A higher hierarchical planning layer will then leverage encoded manipulation constraints within the robot-head interface to ensure that sensitive H&N structures are not damaged by radiation while the lower collision-free path in the hierarchy is to be executed. This layer of the planning algorithm might need to be repeatedly carried out in a fast computational loop to ensure all $\mathcal{C}$-space constraints are satisfied. Then a higher level plan takes the actions from the two previous lower level plans and generates a robustly stable controller in the sense of Lyapunov such that it can move the head along the $\mathcal{C}_{free}$ paths even in the presence of parametric errors, or uncertainty in model dynamics [20, 55, 56]. **I further hypothesize that the overall hierarchical plan be sequentially structured so that head motion transitions between *planning modes* ($i.e.$ from an initial location $\xi_i \in \boldsymbol{SE}(3)$ to a goal reqgion $\mathcal{Q}_{goal}$) are executed by leveraging online search protocols, which bias search for optimal and feasible paths to a sequence of modes that yield a smooth representation of head motion.** By these hypotheses, *I will address the current gap in geometric manipulation problems under manifold constraints that leave out stability analysis in the feedback control mode of the motion planner. I will achieve this by leveraging a Lyapunov-based stable estimator of the underlying dynamic system in safely generating optimally-robust single modes that guide transitions that precisely move the head.*

Procedure: I will formulate a stable geometrical representation of the underlying dynamical system and bias search toward optimally stable and robust short-task plans by providing an optimality-based method for choosing a control law once an robust control Lyapnov function (RCLF) [57] is known. I will develop an optimally stable and probabilistically-complete multi-modal planner that has broad applications to general multi-modal planning tasks in safety-critical problems in medical robotics.

A. Preliminaries: Let the set of all possible configurations of the head-robot system be $\mathcal{Q}$ in the C-space $\mathcal{C}$ [58]. Suppose that after a number synthesis of the proposed mechanism [59], the dimension of the robot is n. A particular configuration of the robot is defined by $\xi \in \mathcal{Q}$. We assume that the $\mathcal{C}$ is a closed and bounded metric space, and that $\mathcal{Q}$ is a measurable space $(\mathcal{Q}, \mathcal{B}_{\mathcal{Q}})$ for a $\mathcal{B}_{\mathcal{Q}}$ Borel σ-algebra on $\mathcal{C}$, generated from the metric [60]. The set of obstacles to be avoided are a closed set $\mathcal{Q}_{obs}$, which defines the free configuration space $\mathcal{Q}_{free}$, such that $\mathcal{Q}_{free} = cl(\mathcal{Q} \backslash \mathcal{Q}_{obs})$[2]. Our goal is to find a path from ξ_i to some region of interest $\mathcal{Q}_{goal} \subset \mathcal{Q}$, $i.e.$ a continuous injective map $\sigma : [0, 1] \to \mathcal{Q}_{free}$ such that $\sigma(0) = \xi_i$, and $\sigma(1) \in cl(\mathcal{Q}_{goal})$. In addition, a smooth positive definite and radially unbounded function $V(\xi)$ is a control Lyapunov function (CLF) for the head-robot control affine system $\dot{\xi} = f(\xi) + g(\xi, u)$ if

$$\frac{\partial V}{\partial \xi}(\xi) f(\xi) + \frac{\partial V}{\partial \xi}(\xi) g(\xi) q(\xi) \leq -P(\xi) \;\forall\; \xi \neq 0 \tag{2}$$

where $P(\xi)$ is some positive definite function, $u \in \mathbb{R}^6$ is a control input, and $f(0, 0) = 0$.

B. An asymptotically stable in the large and optimal motion-planner: Our goal is to find an optimal collision-free path, c, with respect to a CLF $V(\xi) : \mathbb{R}^n \to \mathbb{R}^d$ such that

[2] $cl(X)$ is the closure of a set, X.

- $V(\xi)$ is positive for all $\xi \in \mathbb{R}^d \backslash \mathcal{Q}_{goal}$; and $V(\xi)$ exhibits a unique global minimum in the target region $\mathcal{Q}_{goal}$, where $V(\mathcal{Q}_{goal}) = 0$;
- as the head moves along any of the trajectories, we must have $V(\xi^{t,n}) > V(\xi^{t+1,n})$, and $V(\xi^{T^n,n}) = 0$; *i.e.* $V(\xi)$ decreases as time increases and $V(\cdot)$ vanishes when the actuators reach steady state after deformation;
- in addition, we require $V(\cdot)$ to satisfy the CLF requirement in (2)
- robust head motion during motion execution shall be guaranteed by devising *robust stabilizability via continuous state feedback* [57], provided that there exists an RCLF on the control-affine system.

We want to choose a control input $u = q(\xi)$ for some function $q(\xi)$ with $q(0) = 0$ so that equilibrium $\xi_e = 0$ of the closed-loop system

$$\dot{\xi} = f(\xi, q(\xi)) \tag{3}$$

is asymptotically stable in the large [61]. The first condition ensures the cost function is a valid Lyapunov function while the second option maintains the stability property in the sense of Lyapunov (*i.e.* $\dot{V}$ being negative semi-definite for all $\xi \in \mathbb{R}^d \backslash \mathcal{Q}_{goal}$. To avoid wasting control energy and missing optimality during motion execution, as is common with the cancellation or domination of nonlinear terms in feedback linearization, the third option will leverage the *inverse optimal stabilization* in a differential game setting based on the pointwise min-norm control law of [57]. This is attractive because rather than solve a Hamilton-Jacobi-Isaacs (HJI) equation for a control law that yields the path c, the pointwise min-norm control law yields a robustly stabilizable and optimal synthesis of the head motion correction problem.

C. Manifold Constraints: It is not enough for us to find a valid path c that is free of collisions. We also want the head motion to follow constraints that are functions of the robot's geometry, avoids radiation hitting critical structures, follows a path that does not increase proneness to claustrophobia [62], and lower the problem's dimensionality. Similar to [60], we define these *manifold constraints* to capture loop closure constraints, end-effector constraints etc. A forward kinematic map from the configuration of the i^{th} IAB, $\boldsymbol{\chi}_{iab_i}$, maps from respective IAB configurations to head position and orientation $i.e.$ $K_{iab_i} : \boldsymbol{\chi}_{iab_i} \rightarrow SE(3)$. The head velocity with respect to a fixed base frame in terms of IAB velocities can be written in terms of the forward kinematics Jacobian:

$$\begin{pmatrix} v_{iab_i} \\ \omega_{iab_i} \end{pmatrix} = \frac{\partial K_{iab_i}}{\partial \mathbf{r}_i} \frac{d\mathbf{r}}{dt} K_{iab_i}^{-1} = \boldsymbol{J}_i(\mathbf{r}_i)\dot{\mathbf{r}}_i \tag{4}$$

where $\mathbf{r}_i$ is the spatial position of IAB i in generalized coordinates, and $(v_{iab_i}^T, \omega_{iab_i}^T) \in \mathbb{R}^6$ represents the linear and angular velocity of the i^{th} IAB about its screw basis. In essence, $\mathbf{r}_i \in \mathbb{R}^3$ with its rows are mapped to scalars by an appropriate choice of norm[3]. The contact between the head and the IABs is mapped by the Jacobian

$$\boldsymbol{J}_{c_i}(\xi_h, \xi_{iab_i}) = \begin{bmatrix} \mathbf{I} & \hat{\boldsymbol{w}}(r_{c_i}) \\ \mathbf{0} & \mathbf{I} \end{bmatrix} J_{r_i}, \tag{5}$$

where $\boldsymbol{J}_{c_i} : \dot{\xi}_{r_i} \rightarrow \begin{bmatrix} v_{c_i}^T, & w_{c_i}^T \end{bmatrix}^T$, $r_{c_i} \in \mathbb{R}^3$ is a vector between the head reference point (e.g. the center of mass) and the contact with the i^{th} IAB, ξ_h is the position and relative orientation of the head, ξ_{iab_i} is the position and relative orientation of the i^{th} soft robot in world coordinates, $\hat{\boldsymbol{w}}(r_{c_i})$ is an anti-symmetric matrix for the vector r_{c_i}, and $\xi_r = (\xi_{r_1}, \xi_{r_2}, \cdots, \xi_{r_k}), (1 \le k \le n)$ are the positions and orientations for each of the IABs. For $\mathcal{C}^2$-smooth k-constraint functions $G_1, \ldots, G_k$ $(1 \le k \le n)$, a constraint is fulfilled when $g_i(\xi) = 0$ and we write out the composite constraint function $G : \mathbb{R}^n \rightarrow \mathbb{R}^k$ with respect to the contact Jacobians as

$$G_i^T(\xi_h, \xi_{iab_i})\xi_h = B_i^T(\xi_h, \xi_{iab_i})\boldsymbol{J}_{c_i}(\xi_h, \mathbf{r}_{r_i})\dot{\xi}_{iab_i} \tag{6}$$

for an IAB's selection matrix $B_i^T(\xi_h, \xi_{iab_i}) \in \mathbb{R}_i^m$, where m_i is the range of all the forces and moments for the chosen contact primitive (or union of contact primitives). Therefore, for k actuators in the soft robot, we have the following manipulation constraint

$$\begin{bmatrix} G_1^T \\ \vdots \\ G_k^T \end{bmatrix} \begin{pmatrix} v_h \\ w_h \end{pmatrix} = \textbf{diag} \begin{pmatrix} B_1^T \boldsymbol{J}_{c_1} \\ \vdots \\ B_k^T \boldsymbol{J}_{c_k} \end{pmatrix} \begin{pmatrix} \dot{\mathbf{r}}_{iab_1} \\ \vdots \\ \dot{\mathbf{r}}_{iab_k} \end{pmatrix}. \tag{7}$$

The details of this derivation are presented in my unpublished work [28]. We call $\mathcal{M}_{free}$ the free constraint manifold of the overall manifold, $\mathcal{M}$, which is defined as $\mathcal{M}_{free} = \mathcal{M} \cap \mathcal{Q}_{free}$.

Problem 1 (Constrained RCLF Motion Planning)**.** *Find an RCLF collision-free path* $\sigma^\star : [0,1] \rightarrow \mathcal{M}_{free}$ *given a path planning problem* $(\mathcal{Q}_{free}, \xi_i, \mathcal{Q}_{goal})$*, manipulation constraint, G, and cost function V such that* $V(\sigma^\star) = \min_{\sigma \in \Sigma_{\mathcal{M}_{free}}} V(\sigma)$ *if one exists.*

[3] I used the $l2$-norm im my implementation.

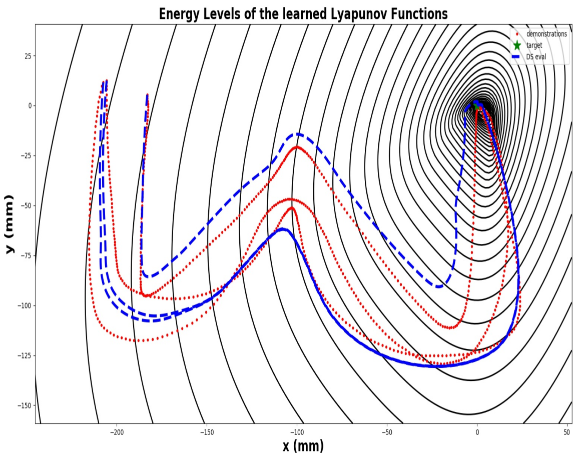

(a) Reproducing a nonlinear W-shape motion

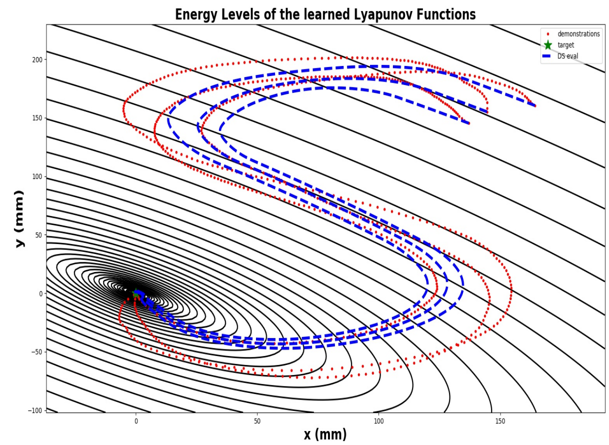

(b) Reproducing a nonlinear S-shape motion

Figure 10: A CLF motion executor (red curves) that shows convergence to local attractors (green asterisks) and follows 3 different set trajectories (blue curves) for 2D nonlinear motion-trajectory problems on the WAM robot.

Expected results: Previously, the stabilizing command for items 1 and 2 in subsection B above was computed by solving a constrained optimization problem to choose the collision-free stabilizing command among the possible solutions. My implementation takes a greedy approach using the L-BFGS optimization algorithm with box constraints, in contrast to the quadratic nonlinear constrained optimization used by [63], to find the minimal value of the control law u at each time step such that u it is stable. Results of this implementation on toy robot nonlinear control from example demonstrations in 2D task space, implemented in python (see [64]), are reprinted in Fig. 10. When the problem identified in Prob. 1 is solved, I should expect my results to provide better trajectory tracking than the non-RCLF implementation I implemented in [64] owing to the account for all possible manifold constraints in the problem formulation.

K_{99} **Aim III: Mechanism Assembly. Phantom and Healthy Volunteer Experiments.**

Rationale.

Case for a parallel soft manipulator: Open-loop kinematic chains have a low transportable load and poor accuracy since the weight of the segments that follow each link and the load of the structure contributes to the large flexure of torques; their links magnify errors from shoulder out to the end-effector, consequently hampering their use for sophisticated control strategies that may minimize or eliminate load-dependent error. Thus, most serially-joined manipulators are stiffened during the manufacturing process – thus, inherently exhibiting a high load-to-weight ratio and a complicated actuation system. Moreover, their passive bending stiffness overwhelms the degree of deformation. Parallel configurations, in spite of their higher number of actuated joints, distribute the weight of the load around the links of the robot, improve manipulation accuracy, have a desirable lightness property (albeit at the expense of a reduced workspace), and minimize the flexure torques that are otherwise common with open-loop kinematic chains. Given the non-cummulativeness of actuator errors in parallel configurations, greater precision is possible with minimal control-complication [65].

Hypothesis.

Owing to the success of parallel robot mechanisms at precise manipulation tasks [2, 20, 66–68], **I hypothesize that a parallel soft-manipulator mechanism will yield the desired submillimeter and subdegree accuracy necessary for online, real-time head motion control in MRI-LINAC RT.**

Procedure.

A. Head Motion Correction in $\mathbb{SE}(3)$: I will systematically synthesize and analyze parallel soft robot manipulators for head and neck motion correction in MRI-LINAC systems. I will then leverage the kinematics and kinetics of soft manipulators which I proposed in [28] to construct the hierarchical motion planner in Aim II. Synthesizing multi-DOF parallel soft robots is challenging given the inter-dependency of the parameters that characterize the deformation, the individual robot constraints' relative three dimensional orientation, permitted motion orientations, the three dimensional relation between constraints and allowed motions, and the possibility of multiple assembly modes that may result in the same end-effector pose [66]. The configuration that shall be investigated shall consist of soft actuators so arranged that their independent or coupled actuation can produce the needed head motion correction along the left-right (LR), the anterior-posterior (AP) , and/or the ssuperior-inferior (SI) axes. I will analyze the manipulation map, kinematics and kinetics of the respective closed-loop chains, and analyze the contact equations between the IAB system and head.

Fig. 11b shows an example standalone motion correction prototype for an IMRT system while Fig. 11c shows the proposed mechanism for MRI-LINAC systems (without MRI coils). Owing to the modular design, the coils of an MRI can be easily integrated onto

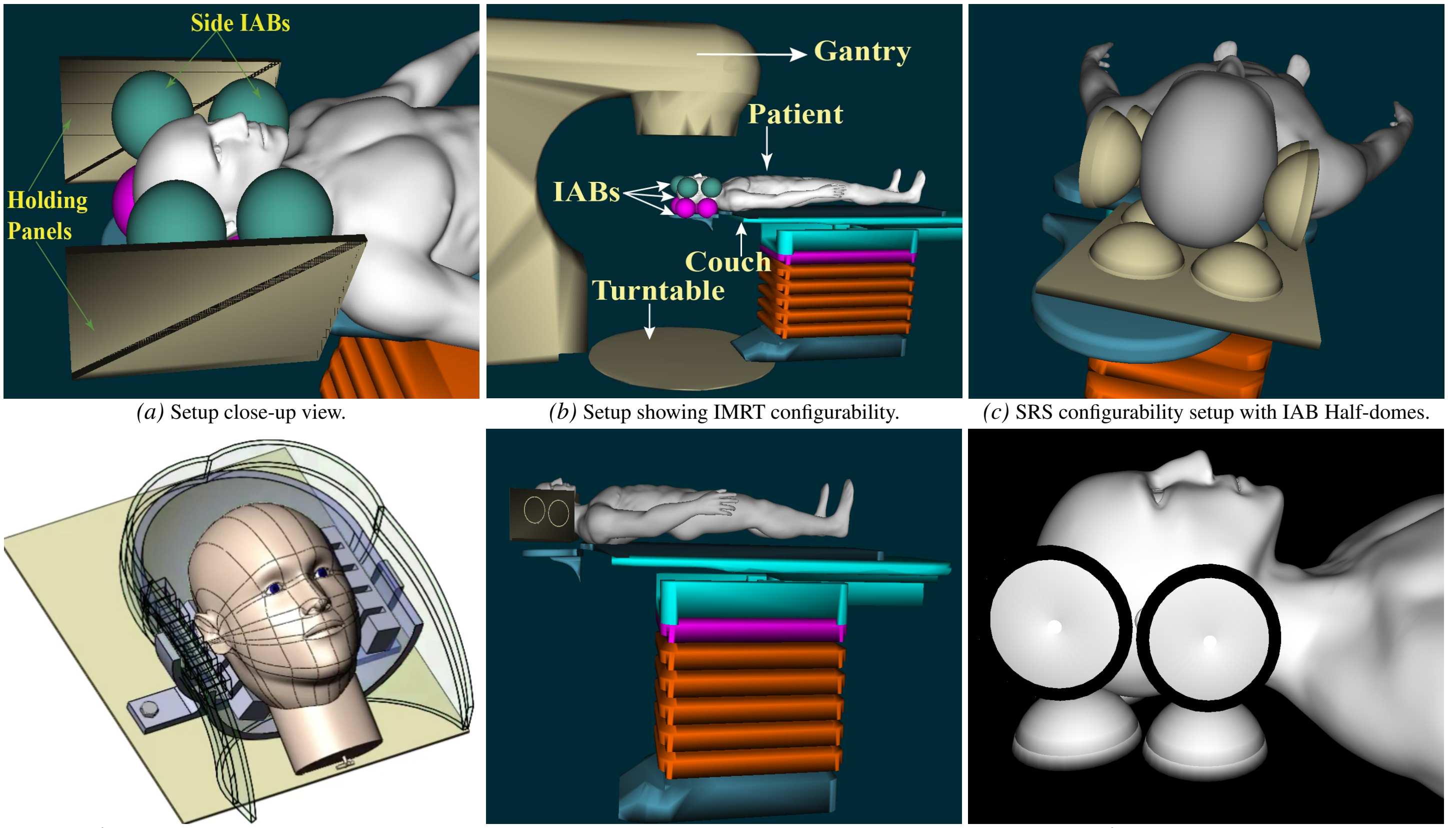

(a) Setup close-up view. *(b)* Setup showing IMRT configurability. *(c)* SRS configurability setup with IAB Half-domes.

(d) Wearable setup under MRI Coils. *(e)* Patient, IABs holders and couch. *(f)* Patient-Robot System.

Figure 11: Proposed MRI-compatible LINAC patient motion compensation system.

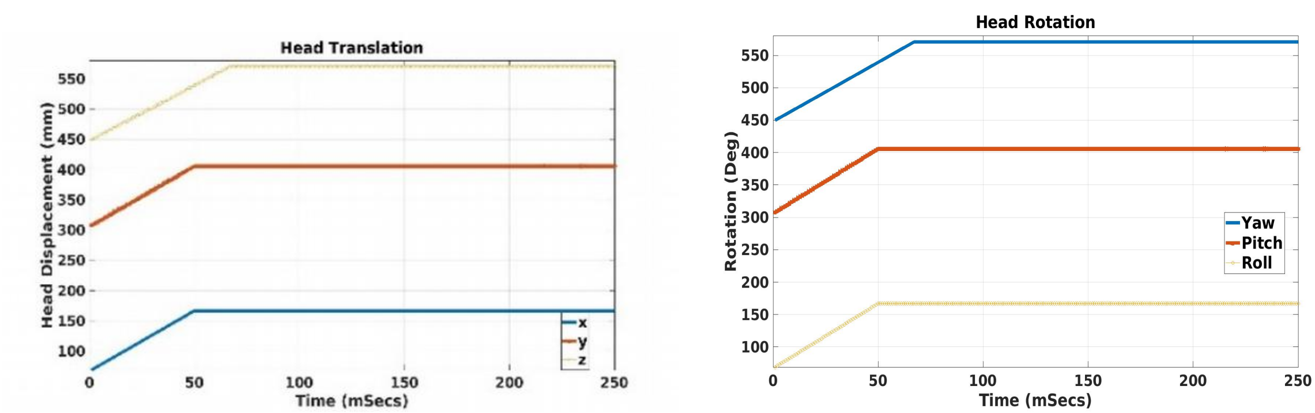

(a) Translational motion. *(b)* Rotational motion.

Figure 12: Open-loop setpoint-following for patient's head motion in $\mathbb{SE}(3)$. Reprinted from [13].

this mechanism. In a parallel kinematic manner, the soft domes are positioned around the patient's cranial region while the patient lies supine on a typical MRI/RT treatment couch (Fig. 11b). The soft domes will be held in place around the head by impact-resistant low-temperature rigid PVC foam insulation sheet that is encased in carbon fiber. Velcro stickers (not shown) will be affixed to the planar soft dome holders to accommodate different patient cranial geometry – thus providing a modularization that ensures re-usability for different patients. The side actuators will correct head motion along the LR axis of the head anatomy $i.e.$ (yaw and roll motions), while the bottom ones will correct head motion along the AP direction. The SI motion will be adjusted by the two lower actuators on the bottom of the neck. These will conform deformation in a non-Gaussian fashion through an appropriate configuration of fiber-reinforcing (see videos). The domes underneath the forehead would control pure z translation and pitch rotasry motions.

In preliminary work [28], I have synthesized differential kinematics [69], continuum mechanics [70,71] and multi-bodied kinematics. Equation (7) yields the cranial manipulation constraint between the soft actuators and the head so that we can find the respective translational and rotational head velocity components, v_h, ω_h respectively in world frames. We can easily find the pseudo inverse of the manipulation map, G in (7), so as to determine head velocity on the treatment couch. The derivation of this equation is detailed in [27].

B. Expected Results: I would expect that my results will follow the open-loop head motion control simulation results in the SOFA [72] framework as presented in my recently accepted publication [13] using the proposed setup of Fig. 11f: raising or rotating the head in $\mathbb{SE}(3)$ resulted in steady-state reference trajectory tracking along all 6-DoFs of head motion as shown in Fig. 12.

R_{00} **Aim: Patient oncological clinical trials.**

To verify accuracy of delivered dose, a complete end-to-end evaluation of the robotic MRI-compatible RT system will be conducted using anthropomorphic phantom studies. From the preliminary data (Fig. 3, 5, 12), whereupon excellent agreement was found between head motion and given target trajectory using the adaptive controller proposed in [20]. Once we ascertain the efficacy of this, we will move to healthy human volunteer trials.

Statistical Plan: Phantom-based and healthy human volunteer trials will be conducted after we finish the design and build of the proposed system. A complete end-to-end testing with 3D printed head phantoms containing dosimetric gel will be used to evaluate 3D radiation dose accuracy for both single and multiple target MRI-compatible RT plans. A 20 volunteer study with a mock radiation beam will be conducted in a clinical environment to verify 6DOF head control and patient safety systems. A clinical study on 20 whole brain patients will be performed where validation of method will be determined by a statistical endpoint defining success as to whether or not the 6D intracranial target is ≤ 0.5mm and $\leq 0.5°$ for greater than 95% of the treatment time.

References

[1] Raaymakers, B., Jürgenliemk-Schulz, I., Bol, G., Glitzner, M., Kotte, A., Van Asselen, B., De Boer, J., Bluemink, J., Hackett, S., Moerland, M., et al.: First patients treated with a 1.5 t mri-linac: clinical proof of concept of a high-precision, high-field mri guided radiotherapy treatment. Physics in Medicine & Biology **62**(23), L41 (2017)

[2] Belcher, A.: Patient Motion Management with 6-DOF Robotics for Frameless and Maskless Stereotactic Radiosurgery. Ph.D. thesis, The University of Chicago (2017)

[3] Herrmann, C., Ma, L., Schilling, K.: Model Predictive Control For Tumor Motion Compensation In Robot Assisted Radiotherapy. IFAC Proceedings Volumes **44**(1), 5968–5973 (2011)

[4] Ostyn, M., Dwyer, T., Miller, M., King, P., Sacks, R., Cruikshank, R., Rosario, M., Martinez, D., Kim, S., Yeo, W.H.: An Electromechanical, Patient Positioning System For Head And Neck Radiotherapy. Physics in Medicine & Biology **62**(18), 7520 (2017)

[5] Raaymakers, B., Lagendijk, J., Overweg, J., Kok, J., Raaijmakers, A., Kerkhof, E., Van der Put, R., Meijsing, I., Crijns, S., Benedosso, F., et al.: Integrating a 1.5 t mri scanner with a 6 mv accelerator: proof of concept. Physics in Medicine & Biology **54**(12), N229 (2009)

[6] Mutic, S., Dempsey, J.F.: The viewray system: magnetic resonance–guided and controlled radiotherapy. In: Seminars in radiation oncology, vol. 24, pp. 196–199. Elsevier (2014)

[7] Fallone, B.G.: The rotating biplanar linac–magnetic resonance imaging system. In: Seminars in radiation oncology, vol. 24, pp. 200–202. Elsevier (2014)

[8] Keall, P., Barton, M., Crozier, S., et al.: Linac program, including contributors from ingham institute, illawarra cancer care centre, liverpool hospital. Stanford University, Universities of Newcastle, Queensland, Sydney, Western Sydney, and Wollongong. The Australian magnetic resonance imaging-linac program. Semin Radiat Oncol **24**(3), 203–206 (2014)

[9] Lagendijk, J.J., Raaymakers, B.W., Raaijmakers, A.J., Overweg, J., Brown, K.J., Kerkhof, E.M., van der Put, R.W., Hårdemark, B., van Vulpen, M., van der Heide, U.A.: Mri/linac integration. Radiotherapy and Oncology **86**(1), 25–29 (2008)

[10] Méndez Romero, A., Wunderink, W., Hussain, S.M., De Pooter, J.A., Heijmen, B.J., Nowak, P.C., Nuyttens, J.J., Brandwijk, R.P., Verhoef, C., Ijzermans, J.N., et al.: Stereotactic body radiation therapy for primary and metastatic liver tumors: a single institution phase i-ii study. Acta oncologica **45**(7), 831–837 (2006)

[11] Xing, L., Lin, Z.X., Donaldson, S.S., Le, Q.T., Tate, D., Goffinet, D.R., Wolden, S., Ma, L., Boyer, A.L.: Dosimetric effects of patient displacement and collimator and gantry angle misalignment on intensity modulated radiation therapy. Radiotherapy and Oncology **56**(1), 97–108 (2000)

[12] Chelvarajah, R., Leighton, B., Martin, L., Smith, W., Beldham-Collins, R.: Cranial immobilisationis there a better way? Radiographer **51**(1), 29–33 (2004)

[13] Ogunmolu, Olalekan and Wiersma, Rodney: A Real-Time Patient Head Motion Correction Mechanism for MRI-Linac Systems. J.R. Cameron and J.R. Cunningham Young Investigator Symposium, AAPM/COMP Meeting, The International Journal of Medical Physics Research and Practice. (2020)

[14] Keall, P.J., Mageras, G.S., Balter, J.M., Emery, R.S., Forster, K.M., Jiang, S.B., Kapatoes, J.M., Low, D.A., Murphy, M.J., Murray, B.R., et al.: The Management of Respiratory Motion in Radiation Oncology Report of AAPM Task Group 76 A. Medical physics **33**(10), 3874–3900 (2006)

[15] Takakura, T., Mizowaki, T., Nakata, M., Yano, S., Fujimoto, T., Miyabe, Y., Nakamura, M., Hiraoka, M.: The geometric accuracy of frameless stereotactic radiosurgery using a 6d robotic couch system. Physics in Medicine & Biology **55**(1), 1 (2009)

[16] Liu, X., Belcher, A.H., Grelewicz, Z., Wiersma, R.D.: Robotic stage for head motion correction in stereotactic radiosurgery. In: 2015 American Control Conference (ACC), pp. 5776–5781. IEEE (2015)

[17] Liu, X., Wiersma, R.D.: Optimization based trajectory planning for real-time 6DoF robotic patient motion compensation systems. PloS one **14**(1), e0210,385 (2019)

[18] McNeil, D.G.: M.R.I.'s Strong Magnets Cited in Accidents. The New York Times pp. A–1 (2005). URL https://www.nytimes.com/2005/08/19/health/mris-strong-magnets-cited-in-accidents.html

[19] Ogunmolu, O.P., Gu, X., Jiang, S., Gans, N.R.: A Real-Time, Soft Robotic Patient Positioning System for Maskless Head and Neck Cancer Radiotherapy: An Initial Investigation. In: Automation Science and Engineering (CASE), 2015 IEEE International Conference on, Gothenburg, Sweden, pp. 1539–1545. IEEE (2015)

[20] Ogunmolu, O., Kulkarni, A., Tadesse, Y., Gu, X., Jiang, S., Gans, N.: Soft-NeuroAdapt: A 3-DOF Neuro-Adaptive Patient Pose Correction System for Frameless and Maskless Cancer Radiotherapy. In: IEEE/RSJ International Conference on Intelligent Robots and Systems (IROS), Vancouver, BC, CA, pp. 3661–3668. IEEE (2017)

[21] Ogunmolu, O., Gans, N., Jiang, S., Gu, X.: An Image-Guided Soft Robotic Patient Positioning System for Maskless Head And Neck Cancer Radiotherapy: A Proof of Concept Study. Medical Physics: The International Journal of Medical Physics Research and Practice, Presented at the AAPM Meeting, Anaheim, CA **42**, 3266–3266 (2015)

[22] Ogunmolu, O.P., Gu, X., Jiang, S., Gans, N.R.: Vision-based Control of a Soft Robot for Maskless Head and Neck Cancer Radiotherapy. In: Automation Science and Engineering (CASE), 2016 IEEE International Conference on, Fort Worth, Texas, pp. 180–187. IEEE (2016)

[23] Ljung, L.: System Identification Theory for the User, second edn. Prentice Hall, Upper Saddle River, NJ, USA. (1999)

[24] Ogunmolu, O., Liu, X., Gans, N., Wiersma, R.: Mechanism and Constitutive Model of a Continuum Robot for Head and Neck Cancer Radiotherapy. In: Accepted at IEEE International Conference on Robotics and Automation (ICRA), Paris, France (2020)

[25] Ishizaka, S., Moromugi, S., Kobayashi, M., Kajihara, H., Koga, K., Sugahara, H., Ishimatsu, T., Kurata, S., Kirkness, J.P., Oi, K., et al.: A remote-controlled airbag device can improve upper airway collapsibility by producing head elevation with jaw closure in normal subjects under propofol anesthesia. IEEE journal of translational engineering in health and medicine **2**, 1–9 (2014)

[26] Baskar, R., Lee, K.A., Yeo, R., Yeoh, K.W.: Cancer and radiation therapy: current advances and future directions. International journal of medical sciences **9**(3), 193 (2012)

[27] Ogunmolu, O.P.: A Multi-DOF Soft Robot Mechanism for Patient Motion Correction and Beam Orientation Selection in Cancer Radiation Therapy. Ph.D. thesis, The University of Texas at Dallas; UT Southwestern Medical Center (2019)

[28] Ogunmolu, O.: Kinematics and Kinetics of an In-Parallel-Actuated Soft Robot Manipulator (2020). URL `https://scriptedonachip.com/downloads/Papers/jmr20.pdf`

[29] Hanlon, R.T., Messenger, J.B.: Adaptive coloration in young cuttlefish (sepia officinalis l.): the morphology and development of body patterns and their relation to behaviour. Philosophical Transactions of the Royal Society of London. B, Biological Sciences **320**(1200), 437–487 (1988)

[30] Hanlon, R.T., Messenger, J.B.: Cephalopod behaviour. Cambridge University Press (2018)

[31] Pikul, J., Cohen, I., Shepherd, R.: Stretchable surfaces with programmable texture (2019). US Patent App. 16/161,029

[32] Walker, L.B., Harris, E., Pontius, U.: Center of gravity of human head and neck. In: ANATOMICAL RECORD, vol. 169, p. 448. WILEY-LISS DIV JOHN WILEY & SONS INC, 605 THIRD AVE, NEW YORK, NY 10158-0012 (1971)

[33] Walker, L.B., Harris, E.H., Pontius, U.R.: Mass, volume, center of mass, and mass moment of inertia of head and head and neck of human body. Tech. rep., SAE Technical Paper (1973)

[34] Clauser, C.E., McConville, J.T., Young, J.W.: Weight, volume, and center of mass of segments of the human body. Tech. rep., Antioch Coll Yellow Springs OH (1969)

[35] Mooney, M.: A theory of large elastic deformation. Journal of applied physics **11**(9), 582–592 (1940)

[36] Rivlin, R.S., Saunders, D.W.: Large Elastic Deformations of Isotropic Materials. VII. Experiments on the Deformation of Rubber. Philosophical Transactions of the Royal Society A: Mathematical, Physical and Engineering Sciences **243**(865), 251–288 (1950). DOI 10.1098/rsta.1951.0004

[37] Xu, P.A., Mishra, A., Bai, H., Aubin, C., Zullo, L., Shepherd, R.: Optical lace for synthetic afferent neural networks. Science robotics **4**(34), eaaw6304 (2019)

[38] Zhao, H., OBrien, K., Li, S., Shepherd, R.F.: Optoelectronically innervated soft prosthetic hand via stretchable optical waveguides. Science Robotics **1**(1), eaai7529 (2016)

[39] Muth, J.T., Vogt, D.M., Truby, R.L., Mengüç, Y., Kolesky, D.B., Wood, R.J., Lewis, J.A.: Embedded 3d printing of strain sensors within highly stretchable elastomers. Advanced Materials **26**(36), 6307–6312 (2014)

[40] Wehner, M., Truby, R.L., Fitzgerald, D.J., Mosadegh, B., Whitesides, G.M., Lewis, J.A., Wood, R.J.: An integrated design and fabrication strategy for entirely soft, autonomous robots. Nature **536**(7617), 451–455 (2016)

[41] Keplinger, C., Li, T., Baumgartner, R., Suo, Z., Bauer, S.: Harnessing snap-through instability in soft dielectrics to achieve giant voltage-triggered deformation. Soft Matter **8**(2), 285–288 (2012)

[42] Anderson, I.A., Gisby, T.A., McKay, T.G., OBrien, B.M., Calius, E.P.: Multi-functional dielectric elastomer artificial muscles for soft and smart machines. Journal of applied physics **112**(4), 041,101 (2012)

[43] Firouzeh, A., Higashisaka, T., Nagato, K., Cho, K., Paik, J.: Stretchable kirigami components for composite meso-scale robots. IEEE Robotics and Automation Letters **5**(2), 1883–1890 (2020)

[44] Sedal, A., Memar, A.H., Liu, T., Menguc, Y., Corson, N.: Design of deployable soft robots through plastic deformation of kirigami structures. IEEE Robotics and Automation Letters (2020)

[45] Truby, R.L., Della Santina, C., Rus, D.: Distributed proprioception of 3d configuration in soft, sensorized robots via deep learning. IEEE Robotics and Automation Letters (2020)

[46] Haubert, K., Drier, T., Beebe, D.: Pdms bonding by means of a portable, low-cost corona system. Lab on a Chip **6**(12), 1548–1549 (2006)

[47] Ogunmolu, O., Folkerts, M., Nguyen, D., Gans, N., Jiang, S.: Deep BOO! Automating Beam Orientation Optimization in Intensity Modulated Radiation Therapy. In: Algorithmic Foundations of Robotics, XIII Workshop, Merida, Mexico. Published in Springer's Proceedings in Advanced Robotics (SPAR) book (2018)

[48] Ogunmolu, O., Gu, X., Jiang, S., Gans, N.: Nonlinear systems identification using deep dynamic neural networks. arXiv preprint arXiv:1610.01439 (2016)

[49] Ogunmolu, O., Gans, N., Summers, T.: Minimax Iterative Dynamic Game : Application to Nonlinear Robot Control. IEEE International Conference on Intelligent Robots and Systems (2018)

[50] Sadeghnejad Barkousaraie, Azar and Ogunmolu, Olalekan and Jiang, Steve and Nguyen, Dan: A Fast Deep Learning Approach for Beam Orientation Selection Using Supervised Learning with Column Generation on IMRT Prostate Cancer Patients. Medical Physics, American Association of Physicists in Medicine (2019)

[51] Ogunmolu, O., Sadeghnejad Barkousaraie, A., Dan, N., Gans, N., Jiang, S.: Deep Learning Neural Network for Beam Orientation Optimization. In: International Conference on the use of Computers in Radiation Therapy XVI (2019)

[52] Adler, J.R., Cox, R.S.: Preliminary clinical experience with the cyberknife: Image-guided stereotactic radiosurgery. In: Radiosurgery 1995, vol. 1, pp. 316–326. Karger Publishers (1996)

[53] Ogunmolu, Olalekan, Liu, Xinmin and Wiersma, Rodney: A Motion-Planner for Robot Head Motion Correction in Stereotactic Radiosurgery. ePoster at The AAPM/COMP Meeting, The International Journal of Medical Physics Research and Practice. (2020)

[54] LaValle, S.M.: Planning algorithms. Cambridge university press (2006)

[55] Ioannou, P., Fidan, B.: Adaptive control tutorial. SIAM (2006)

[56] Lavretsky, E., Wise, K.: Robust Adaptive Control with Aerospace Applications. Springer (2005)

[57] Freeman, R.A., Kokotovic, P.V.: Inverse optimality in robust stabilization. SIAM journal on control and optimization **34**(4), 1365–1391 (1996)

[58] Lozano-Perez, T.: Spatial planning: A configuration space approach. In: Autonomous robot vehicles, pp. 259–271. Springer (1990)

[59] Hunt, K.H.: Kinematic Geometry of Mechanisms. Oxford University Press (1977)

[60] Kingston, Z., Moll, M., Kavraki, L.E.: Exploring implicit spaces for constrained sampling-based planning. The International Journal of Robotics Research **38**(10-11), 1151–1178 (2019)

[61] Kalman, R.E., Bertram, J.E.: Control system analysis and design via the second method of lyapunov: Icontinuous-time systems (1960)

[62] Hricak, H., Amparo, E.: Body mri: alleviation of claustrophobia by prone positioning. Radiology **152**(3), 819–819 (1984)

[63] Khansari-Zadeh, S.M., Billard, A.: Learning control Lyapunov function to ensure stability of dynamical system-based robot reaching motions. Robotics and Autonomous Systems **62**(6), 752–765 (2014)

[64] Ogunmolu, O., Thompson, R.S., Dattari, R.P.: Learning Control Lyapunov Functions in Python. https://github.com/lakehanne/lyapunovearner (2020). Accessed February 10, 2020

[65] Hunt, K.H.: Structural Kinematics of In- Parallel-Actuated Robot-Arms **105**(December 1983), 705–712 (1983)

[66] Merlet, J.: Parallel robots. Springer (2015). DOI 10.1007/978-1-4471-4670-4_99

[67] Hopkins, J.B.: Design of Flexure-based Motion Stages for Mechatronic Systems via Freedom, Actuation and Constraint Topologies (FACT). Ph.D. thesis, Massachusetts Institute of Technology (2010)

[68] Hopkins, J.B., Rivera, J., Kim, C., Krishnan, G.: Synthesis and Analysis of Soft Parallel Robots Comprised of Active Constraints. Journal of Mechanisms and Robotics (2015)

[69] Spivak, M.: A Comprehensive Introduction to Differential Geometry. Vol. V. Berkeley: Publish or Perish. Inc. XI (1979)

[70] Treloar, L.R.G.: The physics of rubber elasticity. Oxford University Press, USA (1975)

[71] Truesdell, C.: A First Course in Rational Mechanics, vol. 1. Academic Press, Inc. (1997)

[72] Faure, F., Duriez, C., Delingette, H., Allard, J., Gilles, B., Marchesseau, S., Talbot, H., Courtecuisse, H., Bousquet, G., Peterlik, I., Cotin, S.: SOFA: A Multi-Model Framework for Interactive Physical Simulation. In: Y. Payan (ed.) Soft Tissue Biomechanical Modeling for Computer Assisted Surgery, *Studies in Mechanobiology, Tissue Engineering and Biomaterials*, vol. 11, pp. 283–321. Springer (2012). DOI 10.1007/8415_2012_125

Training in the Responsible Conduct of Research

To instruct postdoctoral researchers in responsible conduct of research, the University of Pennsylvania Biomedical Postdoc Program mandates postdoctoral training in responsible conduct of research. This training consists of both online and in-person components.

Format

First year postdocs are required to complete two introductory online courses designed by the Collaborative Institutional Training Initiative (CITI) at the University of Miami (citiprogram.org). Online courses are intended as a framework for further discussion and development through monthly 90-minute in-person courses in specific topics relating to responsible conduct of research led by faculty members and staff of the university.

Subject Matter

Introductory online courses cover:

- Research misconduct;
- Data management;
- Mentoring;
- Conflicts of interest;
- Publication practices;
- Ethical issues in research; and
- The use of human and animal subjects.

Monthly in-person seminar topics planned for 2020 include (i) collaboration with industry; (ii) ethical issues in genome research; (iii) ethical issues in peer review; (iv) data collection and management; (v) handling conflicts of interest; (vi) responsible laboratory procedures; (vii) University of Pennsylvania policies concerning research integrity and misconduct reporting; (viii) ethical issues in human and animal research; (ix) the mentor/mentee relationship, and more.

Faculty Participation

The RCR seminars are directed by the Biomedical Postdoctoral Program and is led by faculty and staff including professors in the medical and graduate schools, members of the Institutional Animal Care and Use Committee (IACUC), the Institutional Review Board (IRB), as well as staff such as members of the legal department and senior administrators engaged in research compliance efforts. My mentor, Dr. Rodney Wiersma, conducts an annual laboratory-specific RCR session for all lab members. One-on-one training and discussion will also be provided by Dr. Wiersma through supervision of research activities, sharing experience and insight and reviewing scientific issues and ethical challenges associated with my project and related work in the lab.

Duration of Instruction

The University of Pennsylvania's RCR seminars are 90 minutes long, consisting of ∼60 minutes of lecture and ∼30 minutes of faculty/staff led discussion or small group case-study exercises.

Frequency of Instruction

Postdocs must attend at least 8 sessions (12 hours) of these in-person trainings during their tenure at the university.

Facilities and Other Resources

Laboratory. The research described within this application will be carried out in the John Morgan Building (JMB), which is located in the School of Medicine (SOM). The 209,167 square feet building houses the Johnson Pavilion (which contains the biomedical library with ad-hoc 3D printers freely available to students and researchers), Richards Laboratories, Anatomy Chemistry Building and through them to the rest of the Medical Complex. The department of radiation oncology is located less than a mile away in the Smilow center for translational research which houses all biological-related research fellows and faculties as well as staff.

The laboratory is in room 183 in JMB and it is equipped with two fume hoods, three compressed air supply outlets, three vacuum outlets, three gas supply outlets, two double workbenches, two double wall cabinets, and space for up to six researchers. Standard equipment in the lab include drilling machines, general-purpose mechanical cabinets (pliers, drill bits, and such), microscopes, two hand-wash sinks, and a first-aid kit. The lab is also equipped with an FDM 3D printer. The lab includes four double benches and workspace for ten researchers.

Office. As of the writing of this grant, I am the only research staff hat uses the lab. The applicant's mentor has an office which is directly connected to lab work-area. In addition, two similar rooms are connected to the common lab area that are not currently being actively used.

Roberts Proton Therapy Center. Since we are part of the department of radiation oncology, the applicant and his mentor have full access to the Roberts Proton Therapy Center, which is located less than a mile away from JMB in the Smilow Center for Translational Research. The Roberts Proton Therapy Center combines the unmatched expertise of world-renowned radiation specialists with the latest technology and compassionate care. With five treatment rooms and a dedicated research room, the Roberts proton therapy center is the worlds largest center that integrates proton with conventional radiation therapy. As this research proposal is multifaceted with components consisting testing the soft robot under standalone MR machines, RT machines or integrated MRI-LINAC RTs, no other location offers a better support for carrying out the research described in this work. In addition, in my independent years, I can leverage the connection with the Children Hospital of Philadelphia in evaluating the effectiveness of this robot on children going through radiation therapy.

Scientific Environment. Penn provides an outstanding intellectual and scientific environment for the proposed studies. The University offers a unique environment for research in the biomedical science, which significantly impacts on the research enterprise of Penn SOM. The Penn SOM was the first medical school in the United States, has a rich history as a research-intensive institution and continues to be an international leader in the generation of new knowledge and treatment modalities to improve cancer care. The multidisciplinary research at Penn's 12 schools is supported by numerous core facilities, has university wide standard trainings and services. The proximity of the buildings and schools allow for enhanced collaborations between faculty and across schools.

Equipment

The equipment needed to carry out the mentored phase of this research is available in Drs Wiersma and Turner's laboratories, separated apart by only 800 yards on campus.

Laboratory Equipment.

- FDM 3D Printer;
- Instron testing machine;
- Hand tools set including pliers, cutters and snips hammer, spanners, hex keys, nut drivers, screw drivers, wrenches and wrench sets;
- Accessories such as batteries and chargers, crimping tool, and power tool accessories;
- Soldering station including soldering iron, solder, flux, and suction-based solder removal;
- Passive and active electronic components including carbon-film resistors, capacitors, transistors, integrated circuits and electronic prototyping boards;
- Microscope;
- Pneumatic air outlets.